energies

MDPI

Article

Optimization and Control of Renewable Energy Integrated Cogeneration Plant Operation by Design of Suitable Energy Storage System

Ankem V. R. N. B. Manikyala Rao * and Amit Kumar Singh

School of Electronics and Electrical Engineering, Lovely Professional University, Jallandhar 144402, India; amit.20267@lpu.co.in

* Correspondence: amr854@rediffmail.com

Abstract: Cogeneration is preferred mostly in process industries where both thermal and electrical energies are required. Cogeneration plants are more efficient than utilizing the thermal and electrical energies independently. Present government policies in India made renewable energy generation mandatory in order to minimize fossil fuels consumption and to protect the environment. Hence, many cogeneration plants have been integrated with renewable energy generation. However, post-integration effects increase and introduce inefficiencies in the operation of cogeneration systems. In this paper, a case study of an identified typical cogeneration plant where renewable energy is integrated is considered. Post operational effects on the plant due to integration of renewable energy (solar) are studied and by practical experimentation through cost-benefit analysis the break-even point beyond which renewable energy generation introduces inefficiencies is estimated. Next, a systematic methodology is developed based on the heuristic forward-chaining approach technique to establish the breakeven point. An algorithm/flow chart is developed using an iterative method and executed through MATLAB using practical data from the industry. Suggestions for suitable energy storage devices to store renewable energy beyond the breakeven point, based on a techno-economic analysis of energy storage technologies, are made. Further, the battery energy storage system is designed and the capacity is estimated based on the practical solar irradiance data. A rule-based algorithm is developed to control the charge and discharge cycles of battery storage based on predefined conditions. The payback period is estimated based on the expected monetary benefits of proposed energy storage and the economy of the proposed system is ensured. The post-operational issues are resolved by introducing energy storage. The methodology presented in this paper can be a guiding tool for optimization of various renewable-energy-integrated cogeneration systems.

Keywords: renewable-energy-integrated cogeneration systems; heuristic forward approach; breakeven point; energy storage technologies; renewable energy storage

Citation: Manikyala Rao, A.V.R.N.B.; Singh, A.K. Optimization and Control of Renewable Energy Integrated Cogeneration Plant Operation by Design of Suitable Energy Storage System. *Energies* **2022**, *15*, 4590. https://doi.org/10.3390/en15134590

Academic Editor: Ali Mehrizi-Sani

Received: 21 March 2022
Accepted: 30 May 2022
Published: 23 June 2022

1. Introduction

Cogeneration or Combined Heat and Power (CHP) plants simultaneously generate heat and power, both of which are utilized [1]. Normally the electricity generated by cogeneration plants is used for internal consumption, hence saving on transmission and distribution losses. The efficiency of cogeneration plants reach up to around 90% compared to conventional power plants, where maximum efficiency is only 30–38% [1]. Therefore, industries that require both heat and electrical energies have adopted cogeneration. This has made the industries independent in meeting energy requirements with the added advantages of improved reliability in power supply. No revenue drain in the name of grid electricity charges is envisaged. Worldwide electricity reforms like electricity act 2003 in India further encouraged industries to opt for cogeneration. Cogenerators adopted the standard designs available to suit the heat and electrical load requirements. However, rapid

industrialization growth and an increase in energy demand have become a threat to the environment and fossil fuel availability. Most of the state regulatory commissions in India have made it mandatory that at least 6.6% of the total generation should be from Renewable Energy (RE) resources or that equivalent Renewable Energy Certificates (RECs) should be produced through purchase from power exchanges [1]. Hence, over a period, either to meet the statutory requirements of Renewable Power Purchase Obligations (RPPOs) or to minimize electrical energy generation, many industries have gone for RE addition. However, operational issues have developed due to deviation from the earlier standard operating parameters [1].

In their close association with industry, the corresponding author has personally experienced the challenges/problems faced following integration of RE with an existing cogeneration plant. Associated with experiments conducted to establish the conditions responsible for deviation from the optimality conditions. Based on the experiments, it is concluded that the main factors attributed to inefficient operation are reduction of extraction steam flows through turbines resulting in an increase in the heat rate of a turbine, and reduction of steam generator outlet flows to below the threshold values, resulting in oil support and cost escalation [1]. To optimize the cost, it was suggested to the management to restrict solar plant capacity only to the point it does not deviate from the optimality conditions. It is found that only 50% of the installed solar plant has become operative. With the revised operation, the industry is keeping 50% of the solar plant idle and is not able to fully meet the RPPOs obligation. Hence, the main motivation of this research work was initiated from a practical problem faced in the industry; it was decided to innovate a way of fully utilizing the installed solar capacity and to optimize the cogeneration plant's operation. Knowing that a potential outcome of this research could be to resolve major global issues of energy security and environmental degradation in addition to presenting a solution to the many cogeneration plants further boosted the motivation to take up the research with the following objectives,

1. To investigate the challenge of achieving full capacity utilization of RE integrated with existing industrial cogeneration.
2. To establish a Breakeven Point (BEP) beyond which RE utilization becomes inefficient by developing an algorithm using a suitable heuristic technique.
3. To establish a comparative analysis of RE storage options available and determine suitable technique to store RE beyond the BEP.
4. To develop and Simulate Mathematical modeling using MATLAB to balance energy flows including energy storage and discharge devices to maximize RE capacity utilization.

A literature survey was conducted to study the similar problems faced by cogeneration plants with the integration of RE. Most of the literature available focused on challenges related to RE integration with the grid and related to the transmission system. Much literature available on CHP plants focused on stabilization and optimization using thermal energy storage through solar concentrating power, compressed air energy storage systems, battery storage systems, etc. It was suggested by [2] to accommodate the RE generation by transforming district heating demand to electrical demand. Hence, the criteria for meeting thermal energy requirements from the CHP plant are relaxed. Efficiency and profitability improvement by thermal energy storage [3] is envisaged. CHP optimization is preferred through thermal energy storage and discharge during low and high heat demand periods respectively and producing electricity during peak pricing periods [3]. A study on load reduction in CHP plants while maintaining a reliable steam supply process is presented in [4]. The model developed contains a gas turbine, heat recovery SG with supplementary firing, and an extraction condensing steam turbine. Considering technical limitations/constraints on various systems, different operation strategies are developed. However, the system considered has multiple control options like load reduction on gas turbine and steam turbine, and control on auxiliary firing, etc. against only single control of load reduction on a Turbo Generator (TG) in the present case. The study concluded that RE, intermittent by its nature, can be best utilized in tandem with energy storage. By

adopting the same philosophy, a strategy is formulated to utilize the RE generation up to the point where optimal conditions are soundly met. The RE generation above this BEP is planned for storage. The stored energy utilization is planned during non-RE periods. This innovative idea finally resulted in system optimization.

The outcome of the practical experiments resulted in an estimation of BEP beyond which RE utilization makes the system inefficient. As the BEP estimation by practical approach is cumbersome, time-consuming, and may not be feasible, the study was extended to develop the methodology and techniques to estimate the BEP based on theoretical means. To identify suitable heuristic techniques, a literature survey was made [5,6] on various heuristic techniques and the forward approach technique was found to be the most suitable to reach the goal in steps [7].

In the process of developing mathematical modeling, the literature was reviewed to establish theoretical concepts and related governing equations. Literature on cogeneration concepts [8], heat rate establishment of CHP plants [9], thermal analysis of thermal plants [10], and equations governing power generation in turbines [11,12] is extremely helpful in formulating the mathematical equations and developing an algorithm to find BEP by mathematical modeling. Similarly, literature on concepts of internal rate of return/Newton Raphson's empirical formula [13,14] guided precise estimation of the BEP between two RE generation levels with different optimality conditions status. The theoretical method developed based on mathematical modeling is the first attempt based on thermodynamic equations and the same philosophy can be adapted to similar cogeneration plants. The major contribution of this research is the development of a standard theoretical approach to BEP estimation.

Next, a literature survey is made to compare various energy storage technologies (ESTs) available. The literature [15–25] indicated basic concepts and principles involved with each technology. Technical parameters are analyzed to determine the suitability of the storage mechanism. Design limitations and operational constraints are analyzed. Based on the advantages and disadvantages of each technology, the suitability of each technology is assessed and technically feasible storage technologies are suggested. Next, cost comparison of different energy storage technologies on two main approaches viz. Total Capital Cost (TCC) and Life Cycle Cost (LCC) [26] are considered. The main elements of total capital costs include Power Conversion Systems (PCS), storage section, and Balance of Plant (BOP) [26]. LCC accounts for all costs of fixed Operation and Maintenance (O&M), variable O&M, replacement, recycling, disposal, and TCC. A study on Levelized Costs of Storage (LCOS) for three battery technologies namely lithium ion, lead acid, and vanadium flow is carried out in [27] including sensitivity analysis to project the future costs to 2030. Further studies on two energy ratios i.e., the Electrical energy Stored on Invested ($ESOI_e$) and the overall energy efficiency ratio [28] and the data on energy return on investment [29] is accounted to finalize the suitable energy storage option for the present application. An intensive literature survey on technical and financial characteristics resulted in the determination of a suitable storage device for the present application. Hence, another contribution of the research is the development of a methodology to identify suitable storage devices for different applications which can be a guiding tool for many industries.

After identifying suitable energy storage, designing the capacity rating and modeling of energy storage and discharge devices was explored in the literature study. Design and simulation of a PV system operating in grid-connected and stand-alone modes for areas subject to daily grid blackouts are presented in [30], which helped in the estimation of solar power generation from available radiation data. Power and energy rating considerations with the integration of flow battery with solar PV and residential load are presented in [31], which helped in arriving at a battery capacity and rating estimation based on the estimated solar power above BEP. Estimation of solar insulation and power generation of PV systems using previous day weather data [32] and the relationship between solar irradiance and power generated by PV panels [33] are considered for guiding to predict the solar power based on weather data. Modeling of temperature and solar radiation

effects on PV panel power in [34] helped in considering the correction factors on estimated solar power. Modeling, control, and simulation of battery storage PV-wave energy hybrid renewable power generation systems was presented in [35]. Optimal charge/discharge scheduling of battery storage interconnected with residential PV Systems [36] are also considered for modeling the battery storage system. A flow chart is developed to coordinate between frequency support and capacity factor tracking, resulting in behavior closer to a conventional power generation plant in [37]. An energy management strategy for a hybrid stand-alone plant to supply controllable loads is proposed. A fuzzy management algorithm was developed to control a Battery Energy Storage System (BESS) which ensured the maximum use of RE generation in [38]. A rule-based algorithm is developed in a BESS integrated with a solar system, taking into account the operating constraints of the BESS, such as state of charge limits, charge/discharge current limits, and a lifetime of batteries. The algorithm mainly focused on optimal utilization of the BESS so that solar power is dispatched smoothly to supply loads as forecasted [39]. Based on the concepts, a control algorithm was developed to control the charge and discharge cycles of the battery system to the present application.

The storage capacity is determined based on the intensive literature study. Data regarding the solar radiation levels on a minute-wise, hourly, and daily basis is considered from the industry's Automatic Weather Station (AWS) to determine capacity. The cost data of the battery bank is taken from the present market trend and payback and savings are estimated.

The battery energy storage capacity and voltage rating were designed by utilizing the PV power equations. Based on the literature survey on rule-based systems, the algorithm was developed by considering the various conditions for the present application. The charging of the battery bank is considered beyond the BEP of solar generation. The State of Charge (SOC) of the batteries after the completion of discharge is taken as a reference for charging. The amount of charge for every one minute is integrated and rules are defined such that the charging of BESS gets terminated on SOC reaching 100% or completion of the charging cycle. Similarly, the discharge cycle starts based on pre-set discharge timer and the SOC of the BESS is taken as a reference from the final SOC value at the end of the charging cycle. SOC diminishes every 5 min based on the discharge rate at a constant value. The discharge cycle is completed based on predefined rules of either BESS SOC reaching 20% or completion of the discharge timer. The methodology developed takes care of the life of the battery as deep charging or overcharging is not allowed by the algorithm.

Finally, the research resolved the major problems developed in a CHP plant after integration. Estimation of BEP and design of suitable storage capacity to store the RE beyond BEP prevented deviation from optimality conditions. This made the system optimization at full solar capacity possible without affecting the efficiency of the cogeneration plant.

The rest of the paper is organized as follows: Section 2 explains the methodology developed, description of the identified cogeneration plant including the discussion of developed problems, and explores the optimality conditions responsible for inefficient operation after integration. Further, the section deals with the methods/procedures for the determination of BEP through practical experimentation and mathematical modeling. Finally, the various storage technologies available are described, along with each technology's advantages and disadvantages, technical and financial characteristics. Section 3 presents the results based on the developed methods and materials in Section 2, explains a cost-benefit analysis from the data collected through practical experimentation to arrive at BEP including the execution of an algorithm developed to estimate BEP using MATLAB, based on the data available before integration. The section also deals with determining suitable energy storage devices based on the inputs in Section 2. Section 3 also estimates storage device capacity and sizing based on the solar radiation data pertaining to the area. Further, the section discusses an algorithm developed to control storage. Section 4 discusses and compares the results of BEP obtained by both the methods and monetary benefits of storing the RE beyond the breakeven point. The payback period is also presented, to assess

the economic feasibility of the proposed storage device. Finally, Section 5 concludes with an outcome of the research.

2. Methods and Materials

2.1. Methodology

In support of this research work, the case study of a known large-scale process chemical industry situated in the Telangana state of India with location latitude of 17.9312° N and longitude of 80.8266° E is considered. The methodology adopted is indicated in the Figure 1.

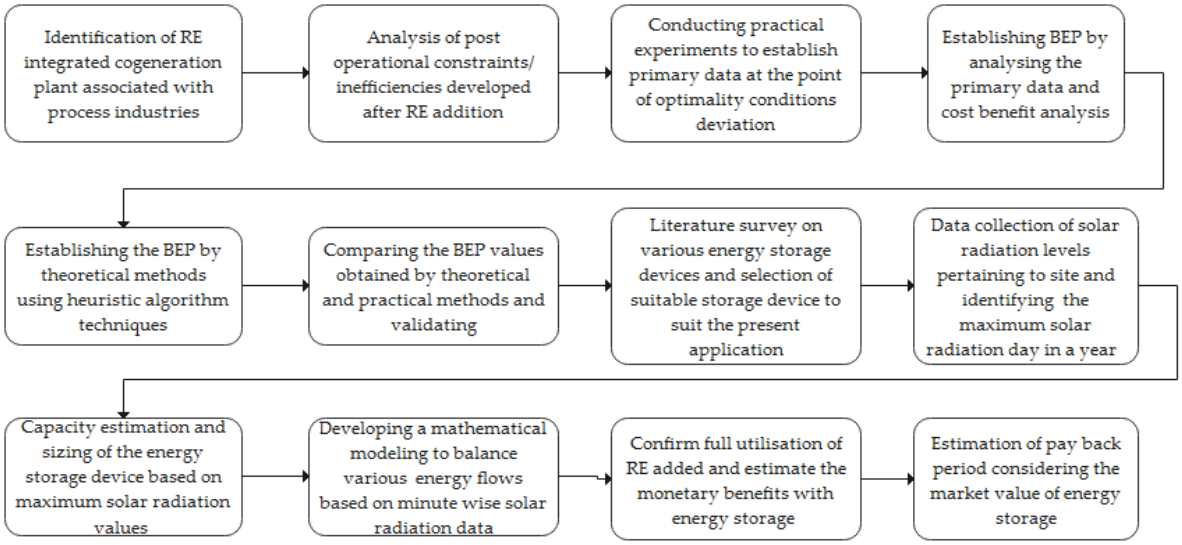

Figure 1. Block diagram of the methodology adopted.

Most of the data and technical details related to the system and equipment are collected from the internal data and through practical experimentation. Complete data such as Steam Generator (SG) and Turbo Generator (TG) flows, steam flow through turbine extractions, and flows through Pressure Reducing and Desuperheating (PRDS) stations of High Pressure (HP) and Low Pressure (LP) steam are recorded. However, it was observed that with full solar utilization, the optimality conditions of SG flows and steam flows through PRDS stations of HP and LP are deviated from, resulting in inefficient operation. To establish the primary data where the optimality conditions starts deviation, experiments are conducted by reducing the generation on TG in steps of 1 Mw and the data is recorded. Reducing the TG generation and correspondingly allowing the import from the grid continued till any one of the optimality conditions deviated. After establishing the deviation from optimal conditions between the two values of TG generation, the final precise value at which optimality conditions are deviating from is obtained by continuing the experiments by decreasing generation in steps of 0.1 Mw between the two values. Theoretically, BEP is obtained by using the developed forward approach heuristic algorithm. The algorithm is developed using the thermodynamic equations and balancing steam flows based on the mathematical model developed. The algorithm is run iteratively until optimality conditions are maintained. The initial data to initiate the algorithm is taken from the data without solar injection into the system. In this way, the data for the purpose of BEP estimation is practically generated. Similarly, the data related to the Global Horizontal Irradiance (GHI) which is the total radiation incident on a horizontal surface, the Global Tilted Irradiance (GTI) which is radiation incident on the tilted plane for the hourly, daily, and monthly data is collected from the AWS provided for the purpose of measurement. The AWS minute-per-minute reported data of various parameters like GHI, GTI, ambient temperature, and solar module temperatures are the basis for the capacity design of storage devices and to establish the energy flows. Hence, most of the primary data is drawn from industry. However, the technical and economic data required for techno-economic analysis to assess

the suitability/selection of storage devices for the present application is derived from the literature survey.

2.2. Description of Identified Renewable Energy Integrated Cogeneration Plant

Figure 2 represents the block diagram of a cogeneration plant where RE is integrated. Here, the solar plant indicated is integrated with the system later and connected to the existing plant's 6.6 Kv switchgear electrical main.

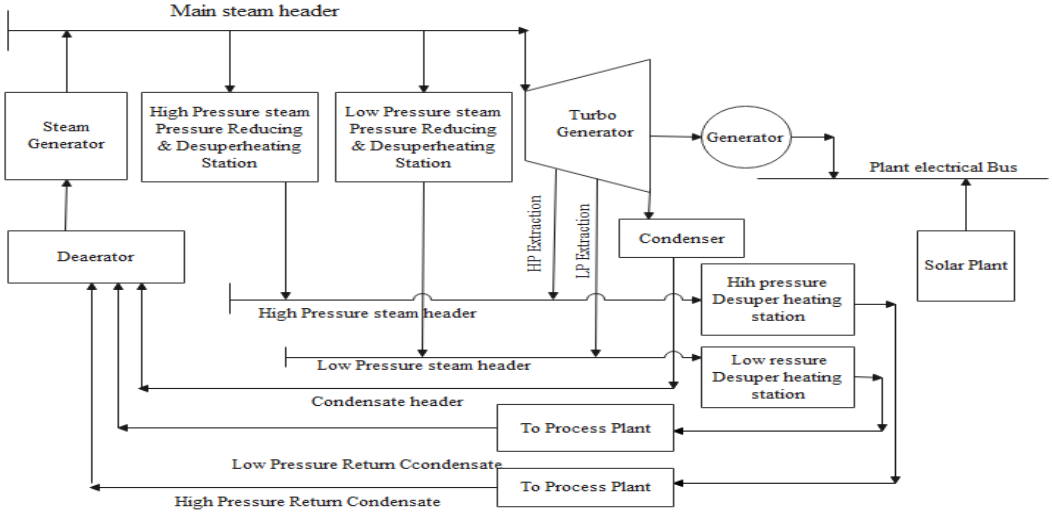

Figure 2. Block diagram of the cogeneration system.

The cogeneration plant of KCR (Kendriya Chemical Refinery) in Telangana state of India is provided with 3 Steam Generators (SGs) each having a capacity of 265 TPH at 106 ata and 485 °C. The steam outlet header of each SG is connected to a common header. Similarly, 3 Turbo Generators (TGs) each 30 Mwe of double extraction cum condensing type supply steam and power. In the block diagram, all 3 SGs and TGs are indicated as a single block. The first extraction, also called HP extraction, is controlled by a turbine governor. LP extraction is controlled through the external control valve. The Main Steam Header supplies steam to TGs, PRDS stations of HP at 32 ata and LP at 8 ata. PRDS supply is used during plant startup and in cases where HP/LP extractions from operating TG units are not sufficient. The temperature of HP/LP going to the process plant is controlled by the HP/LP de-superheating station. Both HP and LP return condensates from the process plant are fed back to the cogeneration plant.

Extraction cum condensing type turbines are provided with power/speed, HP, and LP extraction pressure controls. The master import and export controller maintains the total import or export from or to the grid. The speed/power controller maintains the TG generation constant by operating both HP and LP control valves in the same direction. HP extraction pressure in the controller maintains constant HP steam by operating the HP and LP control valves in the opposite direction. The ratio module determines the ratio of HP and LP control valves opening. Based on variations in HP steam pressure, the HP pressure controller maintains the pressure without impacting power generation. Interlocks to the LP control valve ensure the minimum steam flow through the low-pressure part of the turbine. Quick closing Non-Return Valve in the LP extraction ensures minimum flow to the condenser.

To meet the RPPO obligations SPV (solar power plant) of 12 MWp (DC) is installed. Figure 3 indicates the block diagram of the Grid Integrated 12 MWp solar plant.

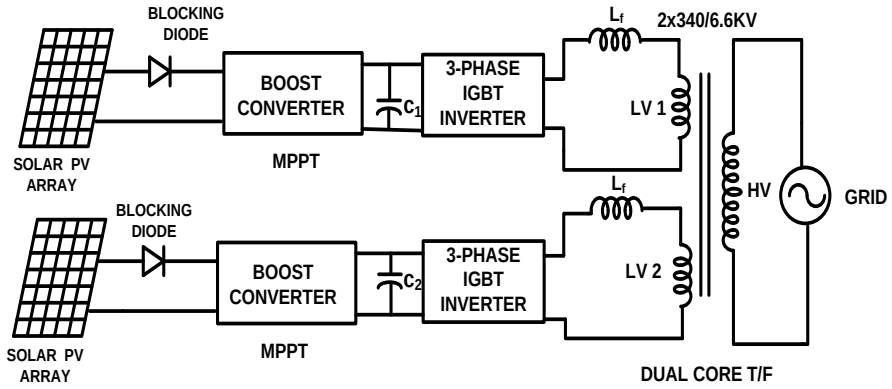

Figure 3. Block diagram of Grid Integrated 12 MWp solar power plant.

The solar plant is connected to a 6.6 Kv switchgear which is connected to the cogeneration plant. A total of 12 MWp is divided into 6 blocks with 2 inverters in each block. The output obtained from the 12 MWp DC systems is divided into two inputs and connected to the process plant substation.

2.3. Operational Constraints Developed after Integration of Renewable Energy

Following are the observations on SG and TG with solar injection.

(a) To maintain no export or import condition, with an increase in solar, the power export/import controller reduces the TG generation. For reducing the power generation from the TGs, the HP control valve goes to a close position, but to maintain constant HP extraction pressure, the LP control valve closes, thereby pressurizing the HP chamber. To maintain LP steam pressure, a control valve external to the turbine adjusts until the margin is available. The reverse phenomenon happens with the reduction of solar generation.

(b) When TG inlet flow declines, the main steam header pressure controller controls the coal feeder speeds to reduce the boiler steam generation. With coal flow variations, the primary air flow varies. Correspondingly the total airflow to the furnace also gets reduced to maintain the flue gas oxygen levels. Hence, furnace disturbances and unburnt residues increase. This increases the system inefficiencies and furnace stability problems.

(c) SG and TG parameter variations are closed cycles in nature. Thus, the cogeneration plant, which was operating very steadily before the integration with the solar plant become unstable and introduced inefficiencies after integration.

Reducing the TG generation below 60% of the MCR (Maximum Continuous Rating) reduces the stage flows drastically and HP and LP are met by corresponding PRDS stations. Supplying the process steam from PRDS stations is uneconomical and reduces the plant efficiency drastically.

The boilers are designed without oil support above 60% MCR only. Whenever the steam generation requirements are declining, oil support is demanded. The oil support at low boiler loads operation increases the steam generation cost.

Hence to obviate the above deficiencies, the cogeneration plant curtails the solar. This is an inefficient operation as the prime purpose of setting up a solar plant is defeated and the RPPOs are not met. This study aimed to resolve the inefficiencies that developed.

Based on the design values/theoretical concepts, the established optimality conditions are [1].

1. Power loss reduction due to reduction of HP and LP extraction flows (X) + throttling loss in PRDS of HP/LP steam, say 2% of X < 0.35% of solar incremental power i.e., if 1.02 X < 0.35% of solar incremental power.
2. Steam flow with SG > minimum threshold value.

Hence, it is worth estimating the BEP, i.e., the point up to which the system can absorb the solar without introducing inefficiencies or becoming uneconomical.

2.4. Estimation of Breakeven Point through Practical Experimentation

It is observed that with the full solar plant in operation, the steam generation falls below the threshold limit of 320 MT/h on both SGs, hence necessitating oil support at both boilers. Hence, experiments were conducted to optimize the plant operation. Instead of allowing the steam flow to fall on both SGs simultaneously, one SG is allowed to run at a constant load of 165 MT/h and the other SG is allowed to absorb the effect of solar generation. In this way only one SG load is falling below the threshold value, necessitating the oil demand on one SG only. From the practical data [1] it is observed that when solar generation is at its peak value, there is a steam demand reduction of 30 MT/h, considering the losses due to part of HP and LP steam flows through corresponding PRDS stations. But the cost analysis proved that the cost incurred due to oil support after accounting for savings in coal due to additional oil support is more than monetary benefits due to the savings in steam reduction. Hence, it is indicated that net savings are lost on account of solar addition.

For this reason, it was decided to keep part of the solar panels equivalent to capacity up to which optimality conditions are not deviated from. In this way, part of the solar generation can be availed without oil demand, meaning no additional costs. To arrive at BEP i.e., beyond which optimality conditions are deviating, the experiments were conducted practically. The entire solar plant is switched off and the panels switched on equivalent to 1 Mw after stabilizing the parameters. The process of adding solar panels in steps of 1 Mw is continued till the optimality condition of SG flow is deviated. It is observed that when 7 Mw equivalent solar panels are in service, the SG flow optimality condition has deviated and the SGs have become unstable. At 6 Mw, solar optimality conditions are maintained. Hence, it is concluded that the optimality condition is deviating between 6 and 7 Mw. To arrive at the exact BEP, the solar panels are taken out in steps of 100 kW and the parameters are observed for any optimality conditions deviation. It is observed that solar optimality conditions are maintained up to 6.3 Mw. Hence, it is concluded that 6.3 Mw is the BEP. Cost-benefit analysis and the practical data collected are presented in the results section.

2.5. Estimation of Breakeven Point through Mathematical Modeling and Forward Approach Algorithm

The manual estimation of the breakeven point involves practically conducting the experiments which are time-consuming and may affect the running plant operation. Moreover, the results depend on maintaining the rated parameters throughout the experiment period. The BEP obtained is applicable to that particular industry only and cannot be correlated with similar plants with different operating parameters. The mathematical model developed is indicated in Figure 4 and Table 1 indicates the variables and constants in the developed model.

Based on the model, equations are developed by considering the various guiding or limiting factors and various controller actions that come into play with solar injection. The equations are executed using the forward approach algorithm. The algorithm is indicated in Figure 5.

With initial stabilized values of the system, the new values are derived based on the developed equations by admitting solar generation/import from the grid in steps of 1 MW. With derived values of various parameters, the optimality conditions are checked for any deviation. If optimality conditions do not deviate, the solar generation/import is again increased by 1 Mw and again checked for optimality conditions. The iterative process is continued till any one of the optimality conditions deviates. The final exact value of BEP is obtained using Newton Raphson's empirical formula [14]. The algorithm developed is executed using MATLAB with the initial data. After the execution of the algorithm, it is found that BEP is 6.8718 Mw based on the steam generator flow falling below the threshold limit of 320 MT/h [1]. MATLAB results are presented in the results section.

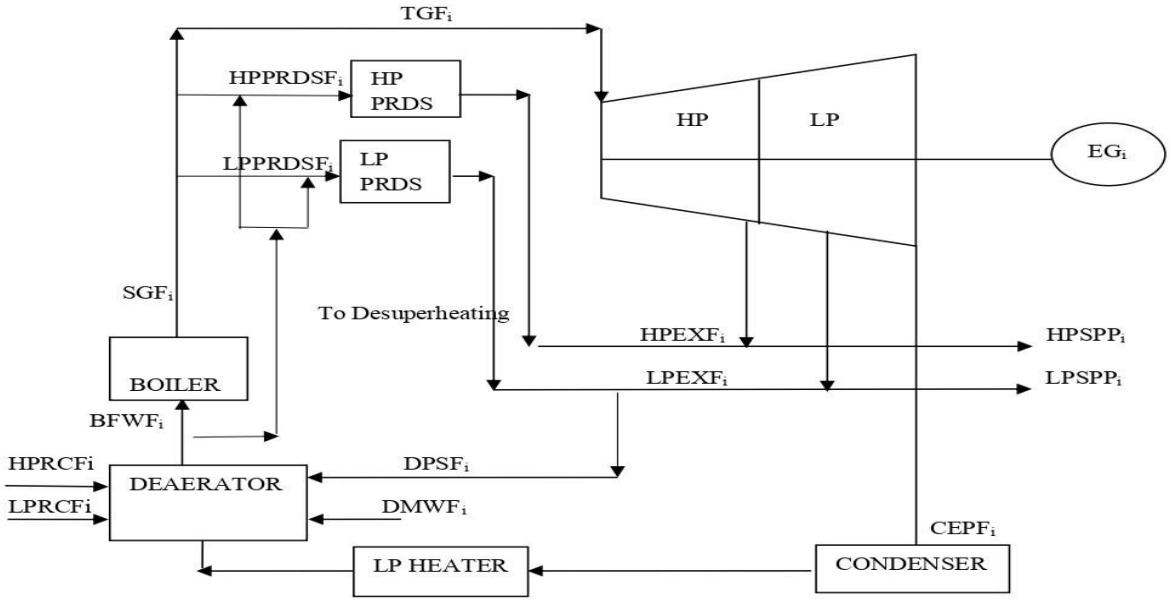

Figure 4. Mathematical modelling of a cogeneration system.

Table 1. Identified constants and variables.

Variables	Constants
SGF_i = Steam Generator Flow at instant i	TGE =Turbo Generator inlet steam Enthalpy at 100 kg/cm^2, 480 °C = 794 kcal/kg
TGF_i = Turbo Generator Flow at instant i	HPSE = Turbo Generator HP Extraction Steam Enthalpy at 32 Kg/cm^2, 347 °C = 747 kcal/kg
HR_i = Heat Rate of a system at instant i	LPSE = Turbo Generator LP Extraction Steam Enthalpy at 8 Kg/cm^2, 238 °C = 694 kcal/kg
SR_i = Steam Rate of a system at instant i	1 Kwh = 860 Kcal
$HPEXF_i$ = HP Extraction Flow through turbine at instant i	DMWE = DM Water Enthalpy = 33 kcal/kg
$LPEXF_i$ = LP Extraction Flow through turbine at instant i	HPRCF = HP Return Condensate Flow =150 MT/h.
$HPPRDSF_i$ = HPPRDS Flow at instant i	LPRCF = LP Return Condensate Flow =20 MT/h.
$LPPRDSF_i$ = LPPRDS Flow at instant i	HPRCE = HP Return Condensate Flow Enthalpy = 235 kcal/kg
$HPPSF_i$ = HP Part Steam flow of a turbine at instant i	LPRCE = LP Return Condensate Flow Enthalpy = 100 kcal/kg
$LPPSF_i$ = LP part Steam flow of a turbine at instant i	DMWE = DM Water Enthalpy = 33 kcal/kg
$PLHPX_i$ = Power Loss in Mw due to steam flow through	BFWE = Boiler Feed Water Enthalpy = 158 kcal/kg
HPPRDS $PLLPX_i$ = Power Loss in Mw due to steam flow through LPPRDS	X = Renewable Energy installed capacity in Mw = 12
PLTXi = Total Power loss in Mw due to steam flow through HP & LP PRDS	
$HPSPP_i$ = HP Steam to Process Plant at 32 kg/cm^2, 238 °C	
$LPSPP_i$ = LP Steam to Process Plant at 8 kg/cm^2, 178 °C	
$DMWF_i$ = DM Water Flow to deaerator	
BEP = Breakeven Point	
GIM_i = Grid Import at instant i	
EG_i = Electrical Generation in MW	
$BFWF_i$ = Boiler Feed Water Flow at instant i	

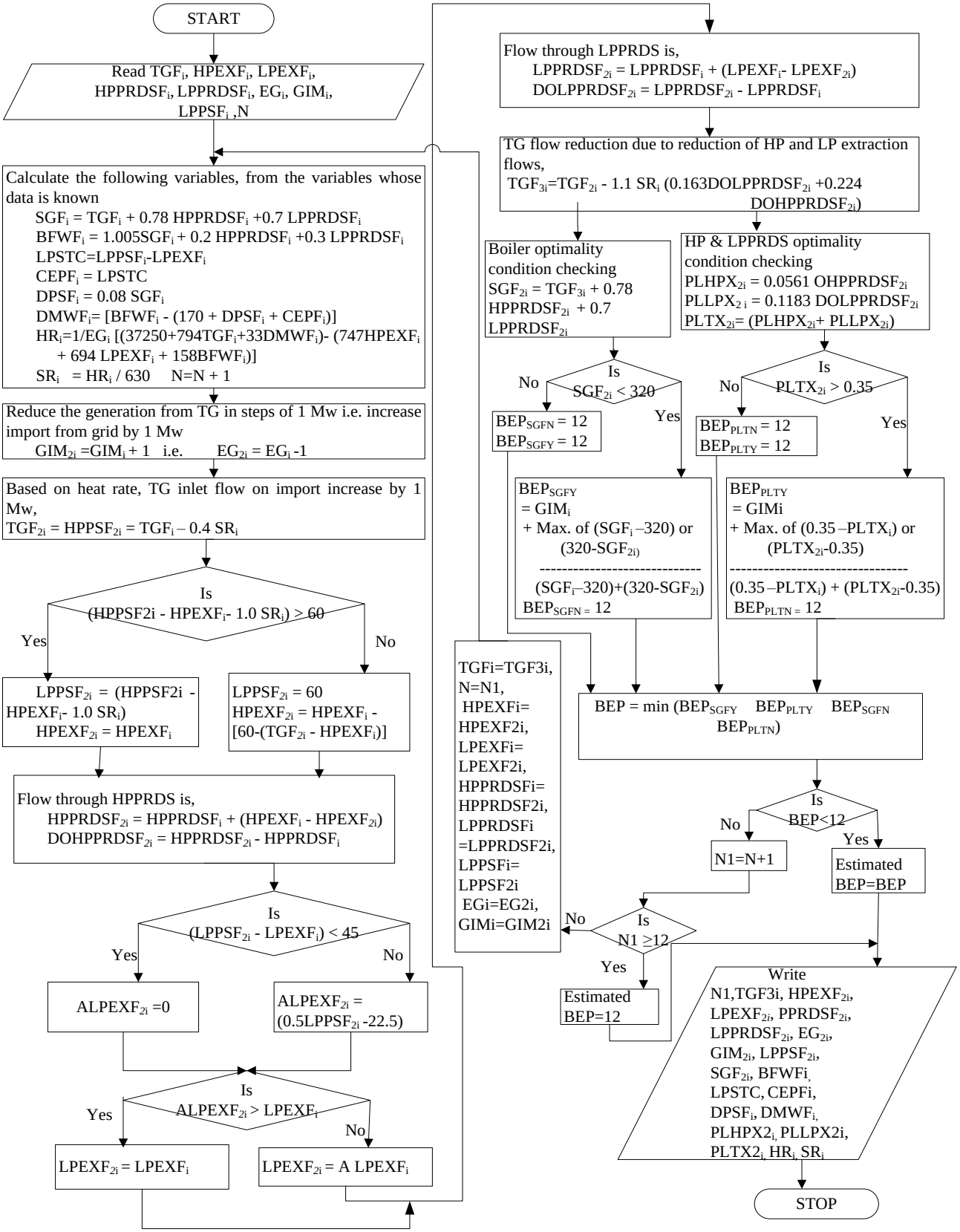

Figure 5. Flow chart to estimate BEP using mathematical modelling.

2.6. Techno-Economic Analysis of Energy Storage Technologies for Selection of Suitable Storage Device

After establishing the BEP, the suitable energy storage device can be selected by carrying out a techno-economic analysis to identify the suitable storage for the present application.

2.6.1. Description of Available Energy Storage Technologies

Energy storage technologies have become popular mainly due to the enhanced utilization of RE in recent days. Due to the intermittent nature of RE, these ESTs have become key components for replacing conventional fossil fuel plants with renewable energy sources (RES). In addition to these, storage devices have become essential in existing cogeneration plants due to post-operational constraints after integration with RE. However, the suitability of the storage device depends on the type of application for which it is required. Hence, the study of storage technologies has become essential, along with a focus on the advantages and disadvantages of each technology. The energy storage technologies can be classified under 5 broad categories based on the form of energy stored and each category can be subdivided as follows.

(1). Electrochemical storage
   i. Lithium-ion battery
   ii. Nickel Cadmium (Ni-Cd) battery
   iii. Sodium sulfur battery
   iv. Lead-acid battery
   v. Redox flow battery

(2). Mechanical storage
   i. Compressed air energy storage
   ii. Pumped hydro energy storage
   iii. Flywheel energy storage

(3). Mechanical storage
   i. Hydrogen
   ii. Methane

(4). Thermal storage
   i. Sensible heat storage
   ii. Latent heat storage
   iii. Thermo-chemical energy storage

(5). Electrical storage
   i. Electrostatic energy storage including capacitors and supercapacitors
   ii. Magnetic/current energy storage including SMES

Another method of classification of energy technologies is by direct and indirect storage [11]. Electrical storage in capacitors/supercapacitors and SMES comes under direct storage. In indirect storage, reservoirs cater to storage. The reservoirs can be either artificial or natural. Batteries and flywheels come the under artificial type whereas pumped hydro and compressed air storage comes under the natural reservoir type.

2.6.2. Electrochemical Energy Storage (ECES)

ECES is the generic name for batteries [15], which are for energy storage usage. Batteries are electrochemical devices with the ability to readily convert the stored energy into electrical energy. Batteries can be in primary or secondary form. Primary batteries are non-rechargeable whereas secondary batteries are chargeable. For large-scale industrial and energy storage applications mainly for RE storage where energy charging and discharging is prime requirement, chargeable batteries serve the purpose. During charging, a direct current is converted into chemical energy, and during discharging chemical energy is

converted back into electron flow in direct current form [17]. Batteries can also be either solid state or flow type [26]. Battery storage does not depend on geographic features [27].

Lithium-Ion Batteries (LIB)

Lithium-ion batteries can be cobalt based or phosphate based. Phosphate-based batteries are a more recent technology and are more efficient than cobalt-based batteries, which require further development [20]. LIB consists of a positive electrode (cathode) of lithium oxides, a negative electrode (anode) of graphite and an electrolyte of a lithium salt and organic solvent [15]. Applicability of LIB is limited to small electronic equipment and not appropriate to stationery applications due to decreased performance and high cost [19]. Low weight and high operating voltage are the main characteristics due to low density of lithium and large electrode potential [15].

Nickel Cadmium

Nickel cadmium batteries are rechargeable batteries using nickel oxide hydroxide and metallic cadmium as electrodes. These batteries offer good cycle life and performance at low temperatures. A significant advantage is the ability to deliver practically their full rated capacity at high discharge rates (discharging in one hour or less). However, the materials are more costly than that of the lead acid batteries and the cells have high self-discharge rates. These batteries are presently used for power tools, portable devices, emergency lighting, telecoms, and generator starting applications and not preferred in large-scale power systems due to high cost and memory effect problems [23].

Sodium Sulphur Batteries (SSB)

Sodium Sulphur batteries consist of two active materials; molten sulfur as the positive electrode and molten sodium as the negative electrode [15]. SSB technology involves high operating temperatures of around 300 °C [16]. Both sodium and sulfur are corrosive in nature, hence prone to corrosion problems. The fact that SSB operates at high temperatures makes it suitable for a large-scale industries like power grids [15]. The Na-S batteries are used for high power energy management such as smoothing the output power, mainly in wind farms, load leveling, and peak shaving [23].

Lead-Acid Batteries

Lead-acid battery technology is the oldest, cheapest, well-developed, widely used rechargeable electrochemical energy storage device, and a popular choice as a backup power supply in a range of kW to tens of MWs [23]. Lead-acid batteries normally consist of lead oxide (PbO_2) cathodes and lead (Pb) anodes immersed in sulfuric acid (H_2SO_4), with each cell connected in series [15]. These batteries operate at ambient temperatures. Operating at lower temperatures increases the life cycle but decreases the rated capacity and the reverse is the case when operating at higher temperatures [16]. Lead sulfate forms on both electrodes during discharge and becomes larger and more difficult to break up during recharging. This necessitates avoiding overcharging or undercharging of these batteries for prolonged periods [20]. These batteries provide a large current with quite low density, which is a great advantage in many applications.

Redox Flow Batteries (RFB)

In Redox flow batteries, pumping of two liquid electrolytes to opposite sides of the electrochemical cell takes place. The two liquid electrolytes contain dissolved metal ions as active masses and they stay dissolved in the fluid electrolyte, hence no phase change of these active masses takes place. The negative and the positive Redox species are contained in separate storage tanks and separated by an ion-selective membrane. Redox-active ions undergo reduction or oxidation reactions when they are in contact or very near to the current collector [15]. The technology is still in the early phases of commercialization compared to more mature battery systems such as Li-ion and lead-acid.

Technical Characteristics of Electrochemical Storage Systems

The technical characteristics of electrochemical energy storage systems are compared in Table 2.

Table 2. Technical characteristics of Electrochemical energy storage systems.

Technical Characteristic	Li-Ion	Ni-Cd	Sodium Sulfur	Lead-Acid	Redox Flow
Capacity [MWh]	0.25–25 [15]	-	≤300 [15]	0.25–50 [15]	≤10 [15]
Power rating [MW]	0.001–0.1 [15]	0–40 [17]	1–50 [15]	0–40 [15]	0.03–7 [15]
Discharge time	Minutes-hours [17]	Seconds-hours	Seconds-hours	Seconds-hours	Seconds-hours
Energy density [Wh/kg]	75–200 [17]	50–75 [17]	150–240 [17]	30–50 [17]	10–30 [17]
Power density [W/kg]	150–315 [17]	150–300 [17]	150–230 [17]	75–300 [17]	-
Efficiency [%]	85–100 [15]	-	75–90 [15]	70–90 [15]	75–85 [15]
Lifetime [Years]	5–15 [17]	10–20 [17]	10–15 [17]	5–15 [17]	5–10 [17]
Cycle life [cycles]	1000–4500 [15]	2000–2500 [17]	2500 [15]	500–1000 [15]	12,000 [15]
Self-discharge per day	0.1–0.3% [17]	0.2–0.6% [17]	≈20% [17]	0.1–0.3% [17]	Small [17]
Storage duration	Minutes-Days [17]	Minutes-Days	Seconds-hours	Minutes-Days	Hours-months [17]
Response time	20 ms-s [23]	20 ms-s [23]	1 ms-s [23]	5–10 ms [23]	s [23]
Discharge duration at max. power	1–8 h [16]	1–8 h [16]	1–8 h [16]	1–8 h [16]	1–8 h [16]
Maturity	Commercialized	Very mature	Commercialized	Mature	Demo [15]
Operating temperature	-	-	-	High 0–100 °F [4]	-
Environment influence	-	-	-	Negative [17]	Negative [17]

2.6.3. Mechanical Storage

In mechanical storage, either potential or kinetic energy is converted into electrical energy by using physical movements. A flywheel is an example of kinetic energy storage, whereas compressed air energy storage and pumped hydro energy storage comes under potential energy storage.

Compressed Air Energy Storage (CAES)

CAES is based on air being pumped by an air compressor run by an electric motor during periods of low demand (off-peak) and the stored compressed air is used to run the turbine to generate electricity during peak periods [15]. Two processes are existing in CAES namely diabatic and adiabatic.

In the diabatic process, during off-peak periods, the air is compressed and the heat generated in the compression process is removed in a heat exchanger (air cooler). The cooled air is stored in an underground storage vessel. During peak periods or when energy is required, the stored compressed air is expanded in a turbine to generate electricity. As the air cools down due to expansion in a turbine, air is heated in a combustion chamber by burning a conventional fuel or biofuel before feeding into the turbine. In this process, as the air is heated by using external fuel, the overall efficiency is less than the adiabatic process.

In the adiabatic process, the heat generated during the compression process is stored to reduce or eliminate the energy loses during the compression process. The stored heat is utilized to heat the compressed air before being admitted into the turbine. As this process is eliminating the additional heat requirement, the efficiency of the storage system will improve considerably.

The compressed air can also be used in gas turbine engines to produce electricity. This is a hybrid compressed air energy system and is like a conventional gas power plant. In a conventional gas power plant, up to 60% of the output from the plant is used to compress air. The remaining 40% is directed to the generator. In a hybrid compressed air system, the stored compressed air removes the need for this, increasing the efficiency of the gas plant up to 70% [22].

Pumped Hydro Energy Storage (PHES)

In PHES systems, water is pumped to an uphill reservoir from a low-level reservoir during periods of low demands. This process is followed by discharging the stored water back to the lower reservoir during periods of peak demands. The discharged water then

drives the generator to produce electricity when needed. The same generator is being used for pumping the water uphill [15].

Flywheel

A flywheel is equivalent to a mechanical battery, simply a mass rotating about its axis which is used to absorb electric energy from the source to store it as rotational kinetic energy and then deliver to a load at the appropriate time, in the form that meets the load requirements [16]. Flywheels are generally used for applications requiring short discharge time, normally for voltage and frequency stabilization [21].

Technical Characteristics of Mechanical Storage Systems

The technical characteristics of Mechanical storage systems are compared in Table 3.

Table 3. Technical characteristics of Mechanical energy storage systems.

Technical Characteristic	Compressed Air Storage	Pumped Hydro Storage	Fly Wheel Storage
Capacity [MWh]	≤250 [15]	≤5000–140,000 [15]	
Power rating [MW]	5–300[15]	<3100 [15]	0–0.25 [17]
Discharge time	1–24 h [17]	1–24 h [17]	ms–15 min [17]
Energy density Wh/kg]	30–60 [17]	0.5–1.5 [17]	10–30 [17]
Power density [W/kg]	-	-	400–1500 [17]
Efficiency [%]	60–79 [15]	65–82 [15]	93–95 [20]
Lifetime [Years]	20–40 [17]	40–60 [17]	≈ 15 [17]
Cycle life [cycles]	8000–12,000 [15]	10,000–30,000 [15]	
Self-discharge per day	Small [17]	Very small [17]	100%[17]
Storage duration	Hours-months [17]	Hours-months [17]	Seconds-minutes [17]
Response time	1–15 min [23]	s-min [23]	<4 ms-s [23]
Discharge duration at max. power	4–24 h [16]	12 h [16]	Minutes–1 h [16]
Maturity	Demo [15]	Mature	Commercializing [23]
Operating temperature	Normal atm [16]	Normal atm [16]	Normal atm [16]
Environment influence	Negative [17]	Negative [17]	Almost none [17]

2.6.4. Chemical Storage

Endothermic chemical reactions absorb energy to form chemical bonds and produce high-energy products. Exothermic reactions release energy, resulting in lower-energy products. Hence, these reactions utilize the stored energy in the bonds of chemical compounds by utilizing electricity and use them for a future energy supply. Hydrogen and methane are two different technologies available [15].

Hydrogen

Hydrogen can be produced either by natural gas reformation or by the electrolysis of water. Even though reforming is more common, electrolysis of water is more convenient from the environmental point of view. The stored hydrogen gets converted back to heat or electricity in an internal combustion engine or a fuel cell [15]. However, the hydrogen and fuel cell combination is a low-efficiency option, as the efficiencies of electrolyzer and fuel cells are around 70% and 50%, respectively [17]. Hence, the overall efficiency and the huge capital costs are major barriers to the commercialization of hydrogen-based systems [26].

Methane

Methane can be produced using hydrogen by a methanation reaction, i.e., the Sabatier process. In the Sabatier process, hydrogen reacts with carbon dioxide (CO_2) and produces methane and water [15], and increases the stability and energy density of the storage media [26].

Technical Characteristics of Chemical Storage Systems

The technical characteristics of Chemical storage systems are compared in Table 4.

Table 4. Technical characteristics of Chemical energy storage systems.

Technical Characteristic	Hydrogen Storage Fuel Cell	Methane Storage
Capacity [MWh]	Varies [15]	Varies [15]
Power rating [MW]	Varies [15]	Varies [15]
Discharge time	Seconds–24 h	-
Energy density Wh/kg]	800–10,000 [17]	-
Power density [W/kg]	500+ [17]	-
Efficiency [%]	20–50 [15]	28–45 [15]
Lifetime [Years]	5–15 [17]	-
Self-discharge per day	Almost zero [17]	-
Storage duration	Hours-months [17]	Hours-months [17]
Response time	Good < 1 s [20]	-
Discharge duration at max. power	Hours as needed [16]	Hours as needed
Maturity	Commercializing [23]	Demo [15]
Operating temperature	50–120 °C [16]	-
Environment influence	Benign [17]	-

2.6.5. Thermal Storage

Thermal energy storage systems can be low or high-temperature systems. The low-temperature systems are further segregated to aquifer low-temperature energy systems, which are not preferable for electricity generation and cryogenic energy storage type, which is only in its development stage [20]. High-temperature systems store thermal energy by heating or cooling a storage medium. The stored energy can be for cooling or for heating applications as well as for power generation. Sensible heat, latent heat, and chemical reactions are the three options available under thermal storage.

Sensible Heat Storage (SHS)

Sensible heat storage store thermal energy by cooling or heating either a liquid or a solid and the capacity of the storage depends on the specific heat of the storage medium [15]. Water tanks and aquifer storage systems are the most common water-based storage systems. In water tank systems, a hot water tank with high thermal insulation avoids thermal losses to store the solar energy via a solar collector.

Latent Heat Storage (LHS)

Latent heat storage stores thermal energy in phase change materials (PCMs). PCM changes phase at a certain temperature called the phase change temperature (PCT), i.e., when the temperature is beyond PCT, the chemical bonds get to break up on a supply of energy (endothermic reaction), and the material changes from solid to liquid. Similarly, as the temperature decrease, the material will return to a solid state by releasing the energy (exothermic reaction). By controlling the temperature rate, it is possible to store the energy. In order to store energy in the form of cold, reverse the process. The storage capacity is greater for LHS than for SHS [15].

Thermo-Chemical Energy Storage (TCES)

TCES refers to storing thermal energy using chemical reactions. When two or more components get combined, releases heat. Similarly, on supplying heat, the compound can be broken and gets divided. The divided components are then stored separately until a demand arises. During peak periods or whenever energy is required, the components are reunited into a chemical compound to release heat. The storage capacity depends on the heat of the reaction. The main constraint with SHS and LHS is heat loss with time. As TCES enables storage for a long duration, it is suitable for large-scale electricity generation. However, TCES technologies are in the development and demonstration stage and further improvements are necessary to make this technology commercially available [15].

Technical Characteristics of Thermal Storage Systems

The technical characteristics of Thermal energy storage systems are compared in Table 5.

Table 5. Technical characteristics of Thermal energy storage systems.

Technical Characteristic	Sensible Heat Storage	Latent Heat Storage	Thermo-Chemical Storage
Power rating [MW]	0.001–10 [15]	0.001–1 [15]	0.01–1 [15]
Discharge time	1–8 h [17]	1–24 h [17]	1–8 h [17]
Energy density Wh/kg]	80–120 [17]	80–200 [17]	150–250 [17]
Power density [W/kg]	-	-	10–30 [17]
Efficiency [%]	50–90 [15]	75–90 [15]	75–100 [15]
Lifetime [Years]	10–20 [17]	5–15 [17]	20–40 [17]
Self-discharge per day	0.5% [17]	0.5–1.0% [17]	0.5–1.0% [17]
Storage duration	Minutes-Days [17]	Minutes-months [17]	Minutes-Days [17]
Maturity	Commercialized [15]	Commercialized [15]	Commercialized [15]
Environment influence	Small [17]	Small [17]	-

2.6.6. Electrical storage

Electrical energy storage can be either in the form of electrostatic like in capacitors and supercapacitors or in the form of magnetic/current storage like superconducting magnetic energy storage [20].

Capacitors

Capacitors store electrical energy in the form of electrical charges accumulated on their plates. However, the stored energy is quickly released from the capacitor as capacitors have low internal resistance. Hence, capacitors are often useful in systems that generate large load spikes [15]. However, capacitors have limited storage potential due to low energy density and are superseded by supercapacitors in large-scale applications [20].

Supercapacitors (Ultracapacitor)

Supercapacitors are the latest innovational devices in the field of electrical energy storage. In comparison with a battery or a traditional capacitor, the supercapacitors have high power and energy density. Normally supercapacitors are electrochemical double-layer capacitors that store energy between two plates or metals and are separated by a dielectric. When voltage is applied across the plates, capacitors work in direct current [15].

Superconducting Magnetic Energy Storage Systems (SCMESS)

SCMESS stores energy in the magnetic field created by the flow of direct current in a coil of cryogenically cooled, superconducting material. When more coils are added to increase the power capacity, coolant is necessary to keep the machine operable, resulting in an increase in cost.

Technical Characteristics of Electrical Storage Systems

The technical characteristics of Electrical storage systems are compared in Table 6.

2.6.7. Economic Characteristics of Energy Storage Systems

Based on the technical characteristics and suitability, the feasible energy systems for a particular application shall be selected. However, to select the most economical storage system from the technically suitable option studying on economic aspects of the storage system is essential. As the present application is for electrical energy storage, a study on cost analysis of Electrical Energy Storage (ESS) systems were considered.

Table 6. Technical characteristics of Electrical energy storage systems.

Technical Characteristic	Capacitors Storage	Super Capacitors Storage	Super Conducting Magnetic Storage
Power rating [MW]	0–0.05 [17]	0–0.3 [17]	0.1–10 [17]
Discharge time	Milliseconds-60 min [17]	Ms–60 min [17]	Milliseconds–8 s [17]
Energy density Wh/kg]	0.05–5	20+ [17]	0.5–5 [17]
Power density [W/kg]	≈100,000[17]	100,000+ [17]	500–2000 [17]
Efficiency [%]	60–65 [20]	90–95 [20]	95–98 [20]
Lifetime [Years]	≈5 [17]	10–30 [17]	20+ [17]
Cycle life [cycles]	50,000+ [17]	100,000+ [17]	100,000+ [17]
Self-discharge per day	40% [17]	20–40% [17]	10–15% [17]
Storage duration	Seconds-hours [17]	Seconds-hours [17]	Minutes-hours [17]
Response time	Very fast [20]	8 ms [23]	<100 ms [23]
Maturity	Developed [20]	Commercializing [23]	Commercializing [23]
Environment influence	Small [17]	Small [17]	Negative [17]

Based on cost analysis of ESS systems, two main approaches were considered, i.e., Total Capital Cost (TCC) and Life Cycle Cost (LCC) [26]. Normally the TCCs of EES systems mainly consist of the purchase, installation, and commissioning of an EES unit comprising a Power Conversion System (PCS), Energy storage section, and balance of plant (BOP). PCS may consist of power interconnection equipment for charging and discharging with different characteristics and the storage section mainly include the storage medium containment equipment like battery banks, air tanks (CAES), reservoirs (PHS), etc. [26]. The BOP may include project engineering, grid integration facilities, monitoring and control equipment, etc. Normally PCS related costs are expressed per unit of capacity i.e., €/kW, whereas energy related costs are expressed per unit of energy stored or delivered, i.e., €/kWh, and BOP costs in per unit of power (€/kW) or in energy (€/kWh), where € is used for EURO currency [26].

TCC per unit of output power rating, (Ccap) is as indicated in Equation (1) [26].

$$Ccap = C_{PCS} + C_{BOP} + C_{stor} \times h \ (€/kW) \quad (1)$$

where C_{PCS}, C_{BOP}, and C_{stor} represent unitary costs of PCS, BOP, and storage compartment (€/kWh), respectively, h is the charging/discharging time.

LCC is more appropriate to compare different EES systems, as it accounts for all-expenses like fixed operation and maintenance costs, variable operation and maintenance costs, replacement costs, disposal costs, recycling costs, and total capital costs.

Annualized life cycle costs (ALCC) is the LCC expressed in Levelized annual costs in (€/kW-year) i.e., the yearly payment an organization should maintain for all the services of EES, including loan payments and upfront the capital costs.

Hence, the Levelized ($C_{LCC.a}$)cost can be expressed as indicated in Equation (2) [26],

$$ALCC = C_{LCC.a} = C_{cap.a} + C_{O\&M.a} + C_{R.a} + C_{DR.a} \ (€/kW\text{-year}) \quad (2)$$

where, $C_{cap.a}$ is annualized TCC and expressed by Equation (3),

$$C_{cap.a} = TCC \times CRF \ (€/kW\text{-year}) \quad (3)$$

where,

$$CRF = \text{capital recovery factor} = i\,(1+i)^T/(1+i)^T - 1 \quad (4)$$

where, i is the interest rate during the lifetime T.

Similarly, $C_{O\&M.a}$ is the total annual operation and maintenance costs and presented in Equation (5).

$$C_{O\&M.a} = C_{FOM.a} + C_{VOM} \times n \times h \ (€/kW\text{-year.}) \quad (5)$$

where, $C_{FOM.a}$ = annualized costs of fixed O & M, C_{VOM} = Variable operation and maintenance costs, n = number of discharge cycles per year and h = Yearly operating hours.

Similarly, $C_{R.a}$ is the annualized replacement costs of EES systems and represented by Equation (6),

$$C_{R.a} = CRF \times \sum_{K=1}^{r} (1+i)^{-kt} \times [(C_R \times h)/\eta_{sys}] \ (€/kW\text{-year.}) \quad (6)$$

where r = replacement period in years, C_R = the future cost of replacement in €/kWh, k = Discharge time in hours and ηsys is overall system efficiency for one full cycle at the rated depth of discharge (DOD).

Similarly, $C_{DR.a}$ is the annualized disposal and recycling costs (C_{DR}) that can be calculated using Equation (7),

$$C_{DR.a} = C_{DR} \times [i/(1+i)^T - 1] \ (€/kW\text{-year.}) \quad (7)$$

From the annualized life cycle costs (ALCC), the Levelized cost of electricity (LCOE) can be expressed by Equation (8),

$$LCOE = ALCC/\text{Yearly operating hours} = C_{LCC.a}/(n \times h) \ (€/kWh) \quad (8)$$

If the cost of charging electricity is deducted from the LCOE, the net Levelized cost of storage (LCOS) can be obtained by Equation (9). This way, the cost of employing EES can be calculated despite the price of electricity,

$$LCOS = LCOE - (\text{Price of charring power}/\text{overall efficiency}) \ (€/kWh) \quad (9)$$

The economical characteristics of various electrical energy storage systems are compared in Table 7.

Table 7. Comparision of economic characteristics of energy storage systems [26].

S. No	Electrical Energy Storage System	TCC * (Average Value) €/kW	Fixed O & M Costs Average €/kW-Year.	$C_{O\&M.a}$ (Average Value) €/MWh.	$C_{R.a}$ €/kWh	ALCC ** €/kW-Year.	(LCOE) €/ MWh
1	PHS	1406	4.6	0.22	-	239	120
2	CAESunder	893	3.9	2.2	-	269	134
	above	1315	2.2	3.1		319	159
3	Fly wheel	867	5.2	2.0	-	-	
4	Lead acid	1923	3.4	0.37	172	646	323
5	NaS	2254	3.6	1.8	180	487	244
5	Li-ion	1160	6.9	2.1	369	493 for T & D	617 for T & D
6	VRFB	2512	8.5	0.9	130	706	353
7	Ni cd	1093	10.9	11	525	842	421
8	Super capacitors	229	-	-	-	-	-
9	SMES	218	-	-	-	-	-
10	Hydrogen Fuel cell	3243	25.1	-	-	385 for T& D	481
11	Hydrogen GT	1570	34.7	-	-	333 for T & D	416

* (1) Total capital cost (TCC) of large scale EES system per unit of normal power rating based on Equation (2). (2) The costs are for the typical size of each system which is not the same for all technologies. ** ALCC costs based on 250 cycles per year, 8% interest rate, and 8 h discharge time.

3. Results

BEP estimation through practical experimentation and by mathematical modeling using forward approach algorithm, determination of suitable energy storage device, design and capacity estimation of the storage device are presented in this section.

3.1. Practical Experimental Results to Estimate BEP

The parameters by practical experimentation are tabulated in Table 8.

Table 8. Experimental results at different operating conditions.

S. No	Description	Data Prior to Solar	Data with Full Solar Plant	Data with Solar 6.3 Mw
(i)	2 SGstotal steam generation	330 MT/h	300 MT/h (SG 1/2 165/135 MT/h)	317 MT/h
(ii)	2 TGS total generation	31 MW	19 MW (TG 1/215.5/3.5 MW)	25.5 MW(TG 1/2 13.0/12.5)
(iii)	Auxiliary TG generation	4 MW	4 MW	3.5
(iv)	HP PRDS opening	Nil	105 MT/h	Nil
(v)	LP PRDS opening	Nil	10 MT/h	7.2 MT/h
(vi)	HP steam before/after de-superheating	210/245 MT/h	210/245 MT/h (TG 1 105 MT/h PRDS 105 MT/h)	210/245 MT/h (TG 1& TG2 105 MT/h each)
(vii)	LP steam before/after de-superheating	20/25 MT/h.	20/25 MT/h(TG 1 10 MT/h LP PRDS 10 MT/h)	20/25 MT/h (TG 1 10 MT/hTG 2 8 MT/h LPPRDS 7 MT/h)
(viii)	Condensate flow	85 MT/h	70 MT/h	70 MT/h

3.1.1. Cost-Benefit Analysis When Full Solar Plant in Operation

(a) Total oil consumption for 4 oil guns = 1.2 MT/h (Each oil gun consumes 300 Kg/h).
Total oil cost/hour = Rs 1.2 × 30,000=Rs 36,000/− Cost of oil/MT=Rs. 30,000/−).
(b) Steam generation values before and after solar = (330 − 300) MT/h = 30 MT/h.
(c) Coal consumption/MT of steam = 5 MT.
Hence coal saved due to steam reduction on steam generators = 30/5 = 6 MT/h.
Cost benefit due to coal saving = Rs 6 × 3500/−=Rs17, 500/− (Rs 3500 is coal cost per MT).
(d) Calorific value of oil = 10,000 Kcal/Kg.
Calorific value of coal = 4000 Kcal/Kg Ratio of oil to coal calorific value = 2.5:1.
Hence 4 oil guns oil quantity of 1.2 MT/h is equivalent to 2.5 × 1.2 MT i.e., 3 MT of coal.
Hence coal saving due to oil firing =Rs 3 × 3500/− = Rs 10,500/−.
(e) Net saving due to coal = (c + d) =Rs (17,500 + 10,500) = Rs 28,000/−.
Hence total benefit with full solar plant = (e − a) = Rs (28,000 − 36,000) =Rs − 8000/−.
As the result is negative it indicates loss by going full solar generation i.e., by keeping full solar plant, there is no financial gain.

3.1.2. Cost-Benefit Analysis When the Part Solar Plant in Operation

From Table 1, at 6.3 Mw solar, resultant steam reduction = (330 −317) =13 MT/h.
Hence coal saved due to steam reduction on steam generators = 13/5 = 2.6 MT/h.
Cost-benefit due to coal saving = Rs 2.6 × 3500/− = Rs 9100/−.
Further increase of solar generation results in oil support as steam generation levels of both boilers is at verge (60% MCR), hence uneconomical.
The experiment is further continued to find out the cost savings below the 6.3 Mw and data recorded is presented in Table 9 and graphically in Figure 6.

Table 9. Cost benefit analysis results.

S. No	Solar Generation in MW	Total Steam Generation in MT/h	Steam Reduction on SGs with Solar in MT/h	Cost Saving Due to Steam Reduction in Rs
1	6.3	317	13	9100
2	6.0	320	10	7000
3	5.5	321.6	8.4	5880
4	5.0	319	11	7700
5	4.5	321	9	6300
6	4.0	323.8	6.2	4340

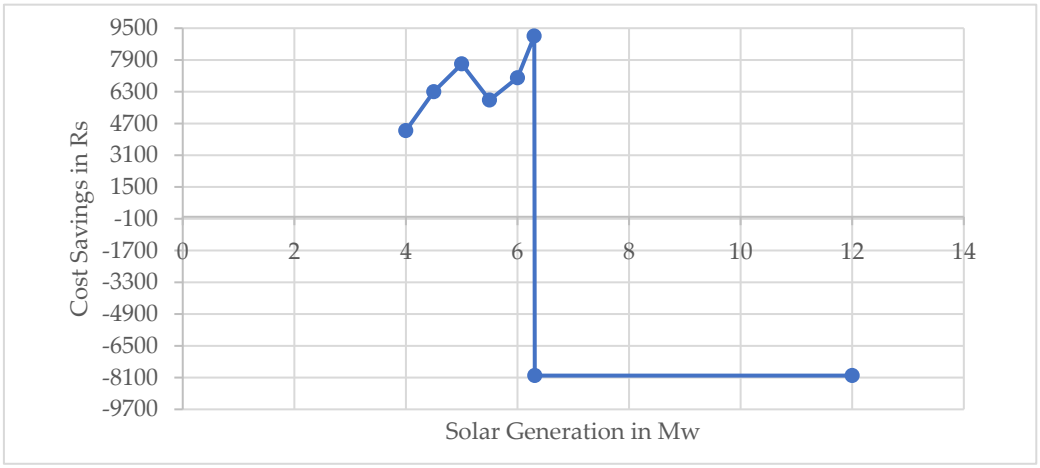

Figure 6. Cost savings in Rs Vs solar generation in MW.

Data indicates the steam reduction on SGs with solar injection and shows an increase up to 13 MT/h at BEP. However, there is a decrease in steam reduction with an increase in solar from 5 Mw to 5.5 Mw as the PRDS station of LP steam started opening. The steam reduction again started increasing with a further increase in solar as the reduction in steam due to solar overrides the effect of PRDS station opening. The savings continued till BEP. From the BEP, even though steam reduction continues till it reaches a maximum reduction of 30 MT/h at full solar, the increase in cost suddenly becomes negative beyond BEP (due to oil support). Hence, it is decided to operate the solar plant up to 6.3 Mw only.

3.2. Mathematical Modeling Results to Estimate BEP

The algorithm developed is executed using MATLAB with the initial data from the industry based on which model is developed. The initial values of variables for the identified RE integrated cogeneration plant are presented in Table 10 and these values are taken after stabilization of the plant without RE injection into the system. Data generated through the MATLAB execution are presented in Table 11.

Table 10. Initial values of variables.

Parameters	EG_i	GIM_i	TGF_i	$HPEXF_i$	$LPEXF_i$	$HPPRDSF_i$	$LPPRDSF_i$	$LPPSF_i$
Unit	Mw	Mw	MT/h	MT/h	MT/h	MT/h	MT/h	MT/h
Initial values	31	0	330	210	35	0	0	120

After execution of the algorithm, it is found that the BEP is 6.8718 Mw based on the SG flow falling below the threshold limit of 320 MT/h. From the data, it is observed that SG flow between 6 and 7 Mw import is falling below the threshold value of 320 Mt/h. Utilizing Newton Raphson's empirical formula [10], the BEP is obtained.

3.3. Determination of Suitable Storage Device Based on Techno-Economic Analysis of Storage Systems

The suitability of each technology with reference to the present case study of a RE integrated cogeneration plant is carried out. Electrochemical storage (battery energy storage systems) is suitable for the present application. The various battery storage devices mentioned have their own merits and demerits. For lithium-ion batteries these are high energy to weight ratio, no memory effect, and long lifetime [20], high discharge rate at maximum power level [21], low self-discharge not exceeding 8% per month [23], and the capability to handle hundreds of charge discharge cycles [16] are the main factors, with limitations such as high expense and relatively low efficiency [21], limited resources of lithium [20] and high temperatures quicken the capacity loss [21], and significant environmental, social,

and health impacts exist [15]. For nickel-cadmium batteries high efficiency, unaffected by DOD, very low maintenance, small self-discharge of 10% per month, operation over a wide range of −40 °C to 50 °C [23] are the main factors with limitations of impact on the environment, and their memory effect problem [23]. For sodium-sulfur batteries long lifecycle, fast response, high recyclability, high pulse power capability [23], high specific energy [15], high energy density [20] and deliver 100% coulombic efficiency [16] are the main factors with limitations being their highly corrosive behavior, high production cost, high operating temperature, and high self-discharge per day [20]. For lead-acid batteries the main contributing factors for consideration are that they can provide high current, high efficiency, high reliability, low self-discharge rate, fast response time, easy recyclability, high specific power, and no block-wise or cell-wise battery management requirement [23], high response to changes in power demand, low standby losses [16], and the maturity of the technology. The main limitations of lead-acid batteries are that they contain toxic substances, have short lifetime, low energy density, poor performance at low temperatures, high maintenance and environmental impact [23], and reduction of capacity at low temperatures [16]. Redox flow batteries have the advantages of short time to fully charge, suitability for large applications with high energy and power density [20], are easy to upgrade [20], have high design flexibility, and can be charged/discharged without loss of capacity. The main limiting factors with this storage are low specific energy, high cost, and their immaturity for utility applications [20], electrical current leakage, and mechanical parts (pumping systems) make system miniaturization difficult [17].

Table 11. Data generated after execution of the algorithm through MATLAB.

Parameters	N = 0	N = 1	N = 2	N = 3	N = 4	N = 5	N = 6	N = 7
SGFi	330	328.6202	327.2553	325.8673	324.4363	322.9539	321.4145	319.8127
TGFi	330	328.6202	326.7955	324.7311	322.5367	320.2426	317.8540	315.3673
HPPSFi	330	328.6202	326.7955	324.7311	322.5367	320.2426	317.8540	315.3673
LPPSFi	120	115.1708	113.6863	111.7538	109.5725	107.2534	104.8272	102.2987
HPEXFi	210	210	210	210	210	210	210	210
LPEXFi	35	35	34.3431	33.3769	32.2863	31.1267	29.9136	28.6494
DMWFi	50.2500	53.8029	53.5650	53.5372	53.6314	53.7676	52.9207	52.4836
HPPRDSFi	0	0	0	0	0	0	0	0
LPPRDSFi	0	0	0.6569	1.6231	2.7137	3.8733	5.0864	6.3506
DOHPPRDSFi	0	0	0	0	0	0	0	0
DOLPPRDSFi	0	0	0.6569	0.9662	1.0907	1.1595	1.2131	1.2643
EGi	31	30	29	28	27	26	25	24
GIMi	0	1	2	3	4	5	6	7
LPSTC/CEPFi	85	80.1708	79.3431	78.3769	77.2863	76.1267	74.9136	73.6493
BFWFi	331.65	330.2633	329.0886	327.9835	326.8726	325.7306	324.5475	321.7179
PLHPXi	0	0	0	0	0	0	0	0
PLLPXi	0	0	0.0777	0.1143	0.1290	0.1372	0.1435	0.1496
PLTXi	0	0	0.0777	0.1143	0.1290	0.1372	0.1435	0.1496
DPSFi	26.4000	26.2896	26.1804	26.0694	25.9549	25.8363	25.7132	25.5850
HRi	2.1731×10^3	2.2203×10^3	2.2687×10^3	2.3214×10^3	2.3775×10^3	2.4369×10^3	2.4999×10^3	2.5750×10^3
SRi	3.4494	3.5243	3.6012	3.6847	3.7737	3.8681	3.9681	4.0873

Compressed air storage is not suitable for the small capacities of the present application as it requires special geological sites, high capital costs, long construction time, requires gas fuel input/gas turbine system, and contaminant emission. Also, this technology is mainly in the demonstration stage and has limited commercial maturity. Pumped hydro storage is also not suitable for the present small-capacity application as normally this device is suitable for high-capacity units of 100–5000 Mw. It has the disadvantages of being location limited, long lead time >10 years, requires special sites for upper and lower water reservoirs, high capital cost, and long construction time. For flywheel storage, even though possessing a better life cycle than batteries, the main drawback is that it provides power for only a few seconds or minutes. Low specific energy, delivery of power for only a few seconds or minutes, safety concerns due to high-speed rotor, energy loss due to friction, relatively low discharge time at maximum power level [21], and high self-discharge rate

are major factors for non-applicability to the present application. This is applicable for high power and short duration requirements.

Hydrogen storage through fuel cells under chemical storage is technically suitable for the present application as it can be stored for a long time, with no emission (coupled to renewable sources) [15]. Normally hydrogen is produced through electrolysis and utilized using fuel cells. The relatively low overall efficiency and huge capital costs are two major barriers to the commercial implementation of hydrogen-based storage in grid-scale applications. Methane storage is by the production of hydrogen produced through electrolysis and converted into methane by reacting with CO_2. But the efficiency is very low, around 33–40%. It is mostly suitable for large-scale applications and not suitable for the present application.

Sensible heat storage, latent heat storage, and thermochemical storage under thermal storage are not suitable for the present application as a 12 Mw solar power plant is established in an existing cogeneration plant to meet RPPOs, hence needing electrical energy storage only and not in the form of thermal energy. Thus, thermal storage can not be used.

Capacitors are limited in their energy storage potential due to low capacity and energy density and also have gradual voltage loss. Hence, they are not suitable for the present application. Even though they show a decrease in voltage and power fluctuations when connected with the grid, supercapacitors are expensive, with low energy density, and also variations in voltage during discharging require power electronics which increases system complexity. Also, the storage period time is seconds to hours only, making it unsuitable for the present application. The main applications of superconducting magnetic storage are for transient and dynamic compensation as energy is released rapidly, resulting in voltage stability. System limitations arise from cooling water requirements. The main constraint for the present application is power availability for a brief period of time. Hence, all the storage devices available under the electrical storage category are unsuitable for the present application.

From the above, it is observed that electrochemical energy storage devices and hydrogen storage through fuel cells are suitable energy storage devices.

3.3.1. Selection of Hydrogen or Batteries for Energy Storage—Net Energy Analysis

To compare regenerative hydrogen fuel cell (RHFC) with battery storage, two energy return ratios i.e., the electrical energy stored on invested (ESOIe) ratio (the ratio of electrical energy returned by the device over its lifetime to the electrical-equivalent energy required to build the device) and the overall energy efficiency (the ratio of electrical energy returned by the device over its lifetime to total lifetime electrical-equivalent energy input into the system) is used. ESOIe depends on characteristics of cycle life, depth of discharge, and cradle-to-gate electrical embodied energy of storage devices [30] ESOIe ratios of various battery storage devices are indicated in Table 12.

Table 12. ESOIe ratios of various battery storage devices and Hydrogen fuel cells [30].

S.No	Energy Storage System	Life Cycle λ	DOD (D)	Cradle-to-Gate Electrical Embodied Energy ε_e	ESOIe $\lambda D/\varepsilon_e$
1	Lithium-ion battery	6000	80	136	35
2	Sodium sulfur battery	4750	80	146	26
3	Lead acid battery	700	80	96	5.8
4	Redox flow battery	2900	100	208	14
5	Zinc bromide battery	2750	80	151	15

ESOIe ratio of the hydrogen fuel cell is 59, the highest compared with battery storage devices. Based on this economic factor, hydrogen storage appears economical. However, the overall energy efficiency of the hydrogen fuel cells is around 33% only, considering the alkaline electrolyzer of efficiency 70% and fuel cell efficiency of 47%. However, the battery energy storage systems overall efficiencies range from 75–90%. Hence, the round-trip efficiency of fuel cell technology must improve dramatically. Thus, for the present application,

only battery storage is the preferred technology. Hydrogen/Fuel cell technology can be thought of with further improvement of efficiency.

3.3.2. Selection of Battery Storage Device Based on Techno-Economic Analysis

Out of the battery technologies discussed, lithium-ion batteries have proven to be advantageous for the electric traction of vehicles, power tools, and intermittently available RE. Applicability of LIB is limited to small electronic equipment and is not appropriate for stationary applications due to decreased performance and high cost [19]. LCOE of Li-ion battery is high compared to other battery technologies, hence not economical. Even though sodium-sulfur batteries have LCOE low compared to other battery technologies, SSB technology involves high operating temperatures of around 300 °C [16], and both sodium and sulfur are corrosive in nature, making them prone to corrosion problems. Flow battery technology is not fully developed and is still immature for utility applications, and LCOE is more than lead-acid batteries. Hence not considered for the present application. Nickel-cadmium batteries are being used currently for power tools, portable devices, emergency lighting, telecoms, and generator starting applications and are not preferred in large-scale power systems due to their high cost and memory effect problems, and LCOE is more than lead-acid batteries. Thus, they are not considered for the present application on techno-economic rounds.

Lead-acid batteries with an LCOE of 323 €/MWh and technically mature technology with many advantages are considered for the application.

3.4. Design of Storage System to Optimize Renewable Energy Integrated Cogeneration Plant

To design and estimate the capacity of a storage system i.e., AH rating of a battery bank, the data of solar radiation levels pertaining to the area is taken as the guiding factor. Table 13 indicates the solar radiation levels of the horizontal and tilted planes in kWh/m^2/day.

Table 13. Monthly average data of solar radiation for one year.

S. No	Period	Total Solar Radiation (kWh/M^2/Month)		Average Radiation (GHI) (kWh/M^2/Day)	Average Radiation (GTI) (kWh/M^2/Day)
		(GHI)	(GTI)		
1	April 2019	189.46	184.57	6.315	6.152
2	May 2019	181.78	167.01	5.864	5.387
3	June 2019	147.79	133.77	4.926	4.459
4	July 2019	127.77	112.5	3.928	3.629
5	August 2019	111.57	106.44	3.597	3.434
6	September 2019	118.21	118.90	3.940	3.963
7	October 2019	144.66	157.02	4.666	5.065
8	Novembr 2019	142.86	170.06	4.762	5.669
9	December 2019	125.76	153.57	4.057	4.957
10	January 2019	135.53	163.92	4.372	5.288
11	February 2019	148.82	167.96	5.132	5.792
12	March 2019	181.11	190.10	5.842	6.132

From the above, it is observed that maximum solar radiation is obtained in the month of April. Hence to estimate the design capacity of the storage system, the day-wise data of GHI and GTI in kWh/m^2 is represented in Figure 7 and the maximum value of daily average solar radiation (GTI) is 6.79 kWh/M^2/Day on 16 April.

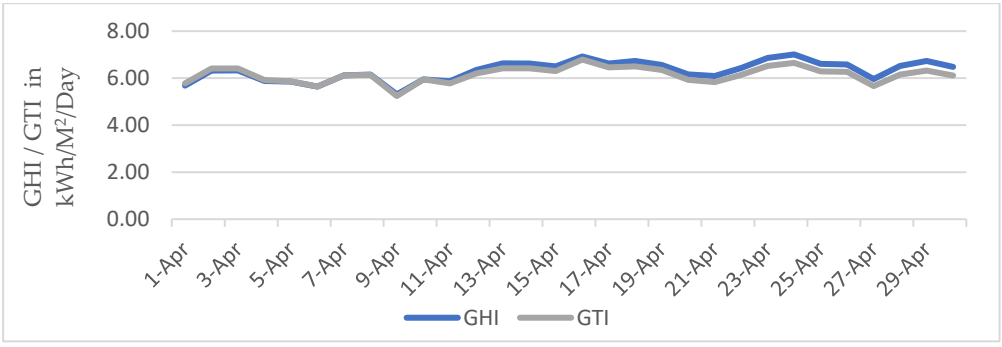

Figure 7. Daily average solar radiation levels in a Month of April 2019.

3.4.1. PV Output Power Estimation using GHI/GTI

Based on the solar radiation per day, the DC power generated from the PV system can be estimated. The DC power generated mainly depends on different factors, including PV peak power at standard test conditions of (STC), solar radiation, and cell temperature and is represented by Equation (10).

$$P_{PVout} = P_{PVpeak} \times (G/G_{ref}) \times [1 + K_t(T_c - T_{ref})] \quad (10)$$

where P_{PVout} is the output power of the PVarray, P_{PVpeak} is the power of the PVarray at STC, G is solar radiation in W/m^2, G_{ref} is solar radiation at STC amounting to 1000 W/m^2, K_t is the temperature coefficient of mono and polycrystalline Si cells amounting to $K_t = -3.7 \times 10^{-31}/°C$, T_{ref} is the reference temperature at STC amounting to 25 °C, and T_C is the cell temperature.

The minute-wise solar radiation is obtained for the maximum data in a year and hourly average values in a day is obtained for 12 h. From the hourly average solar radiation data and the module cell, average temperatures the maximum total power generation for a day is estimated. The solar generation beyond BEP is also estimated and the data is indicated in Table 14.

Table 14. Hourly average data of solar radiation for maximum radiation day in a year.

S. No	Time	GHI (Wh/m^2)	GTI (Wh/m^2)	Average Temperature in °C	Estimated Solar Hourly Average Power in Mwh	Estimated Solar Hourly Average Power in Mw > BEP (6.3 Mw)
1	6.01 a.m.–7.00 a.m.	11.16	12.44	13.88	0.16	0
2	7.01 a.m.–8.00 a.m.	130.41	163.14	19.5	1.99	0
3	8.01 a.m.–9.00 a.m.	345.78	421.08	33.18	4.88	0
4	9.01 a.m.–10.00 a.m.	583.51	586.41	43.55	6.55	0.258
5	10.01 a.m.–11.00 a.m.	741.26	753.43	50.84	8.17	1.87
6	11.01 a.m.–12.00 a.m.	809.46	983.85	51.94	10.63	4.33
7	12.01 a.m.–1.00 p.m.	881.64	1029.49	52.31	11.11	4.8
8	1.01 p.m.–2.00 p.m.	846.55	974.78	52.23	10.52	4.22
9	2.01 p.m.–3.00 p.m.	721.06	827.71	50.03	9.01	2.71
10	3.01 p.m.–4.00 p.m.	516.76	617.24	47.21	6.79	0.61
11	4.01 p.m.–5.00 p.m.	283.37	354.91	39.54	4.02	0
12	5.01 p.m.–6.00 p.m.	56.93	69.65	29.57	0.81	0
	Total	5927.89	6794.13	-	74.64	18.798

Figure 8 indicates the hourly average values of GTI and corresponding generation of the power based on Equation (10). Figures 9–20, indicates the hourly solar power generation and the excess generation available for storage above BEP are plotted based on minute-wise data.

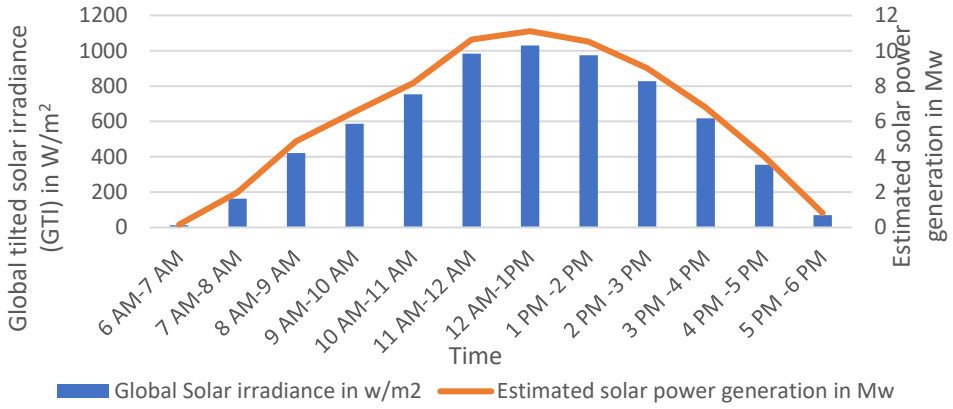

Figure 8. Hourly variations of GTI and solar power generations in a day.

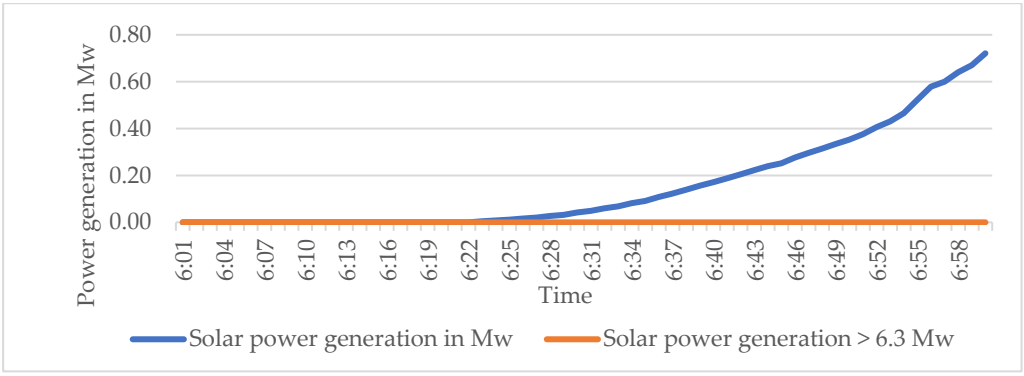

Figure 9. Solar generation between 6:00 a.m.–7:00 a.m.

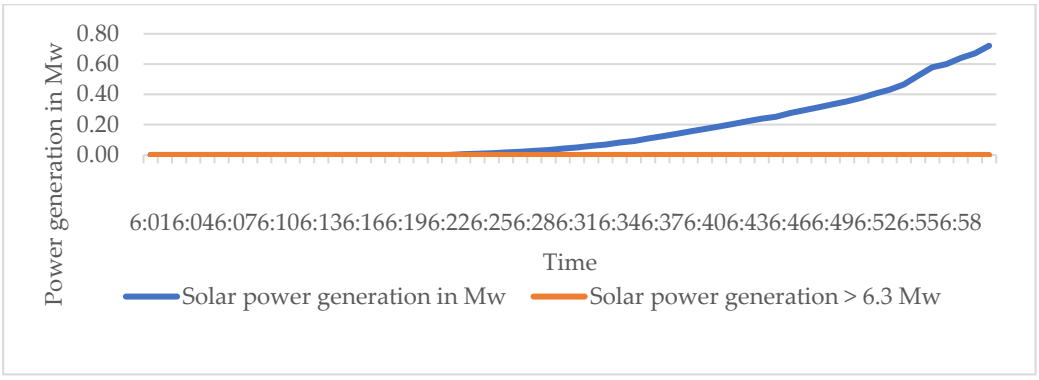

Figure 10. Solar generation between 7:00 a.m.–8:00 a.m.

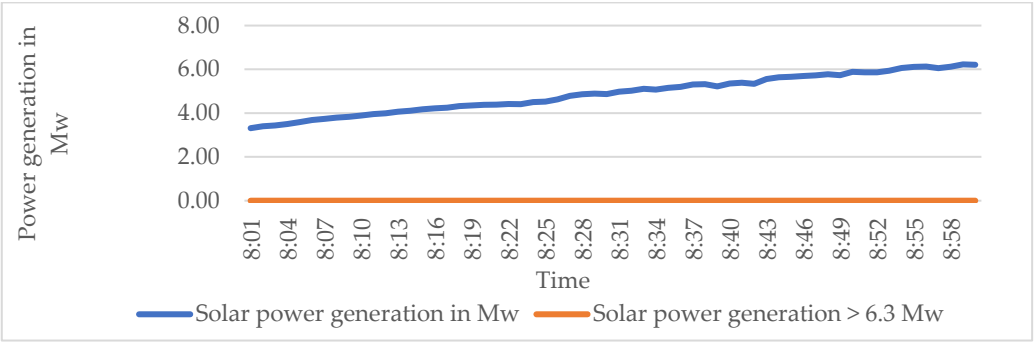

Figure 11. Solar generation between 8:00 a.m.–9:00 a.m.

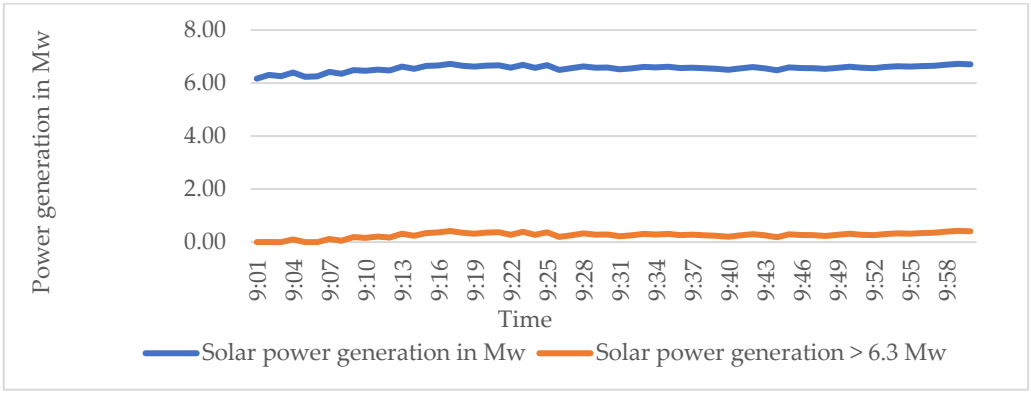

Figure 12. Solar generation between 9:00 a.m.–10:00 a.m.

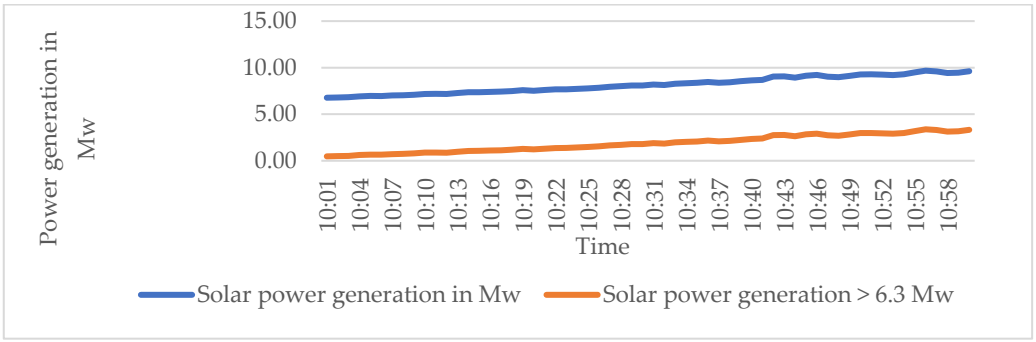

Figure 13. Solar generation between 10:00 a.m.–11:00 a.m.

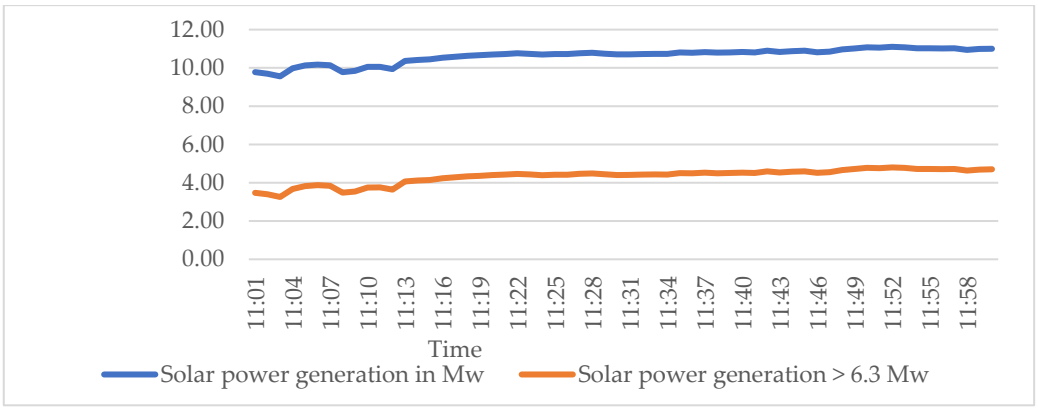

Figure 14. Solar generation between 11:00 a.m.–12:00 a.m.

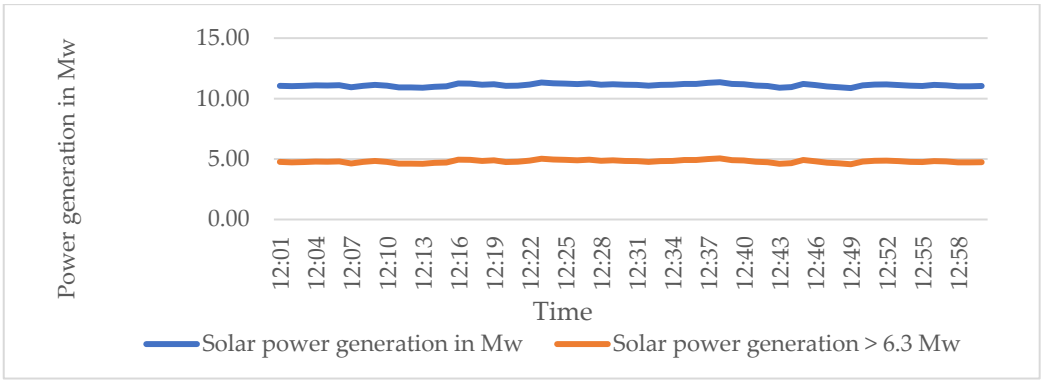

Figure 15. Solar generation between 12:00 a.m.–1:00 p.m.

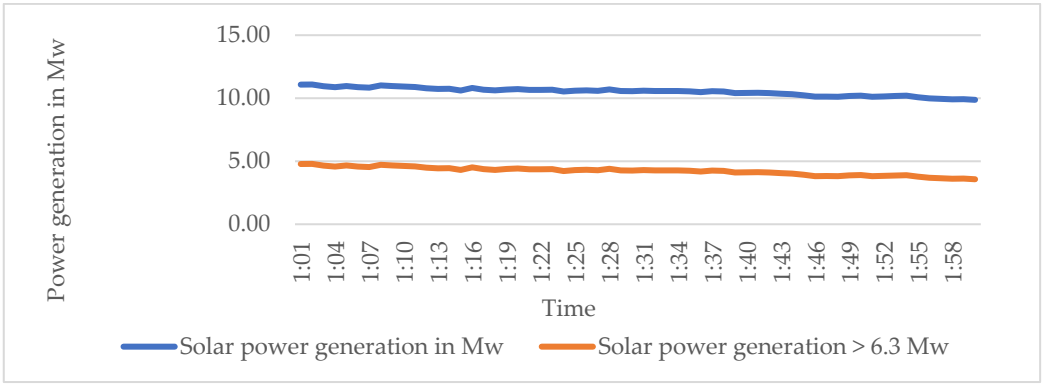

Figure 16. Solar generation between 1:00 p.m.–2:00 p.m.

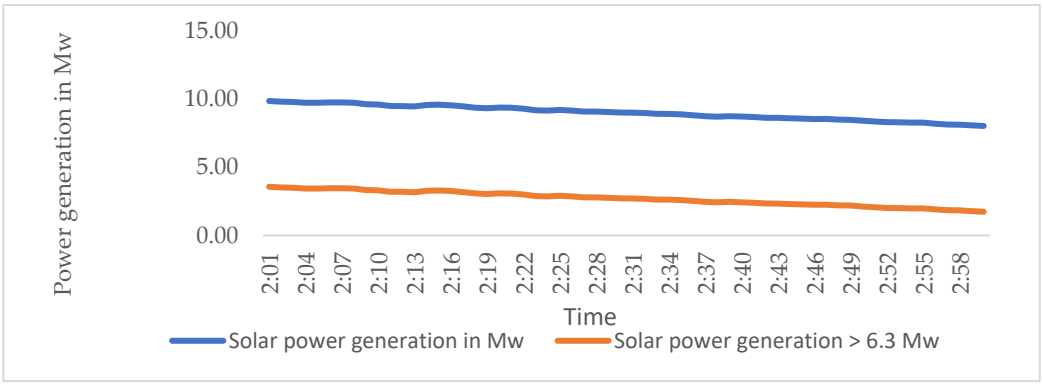

Figure 17. Solar generation between 2:00 p.m.–3:00 p.m.

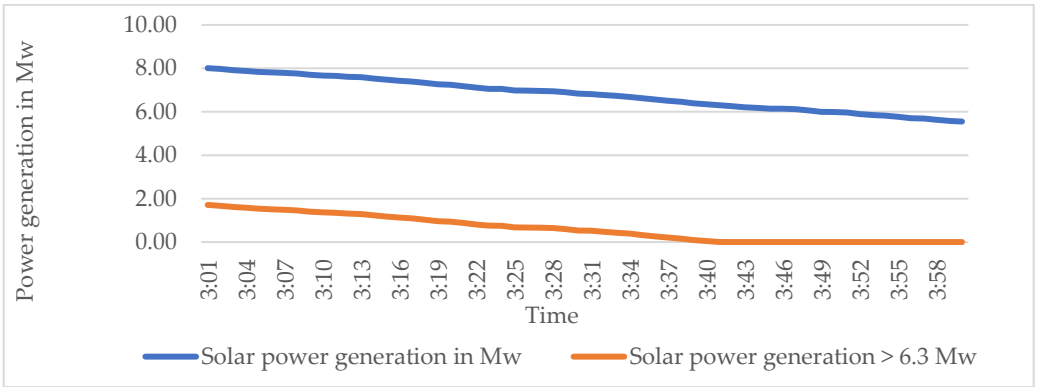

Figure 18. Solar generation between 3:00 p.m.–4:00 p.m.

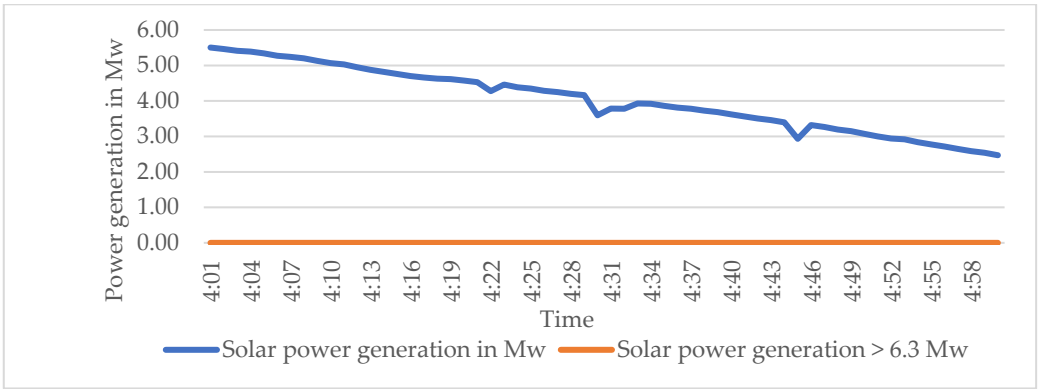

Figure 19. Solar generation between 4:00 p.m.–5:00 p.m.

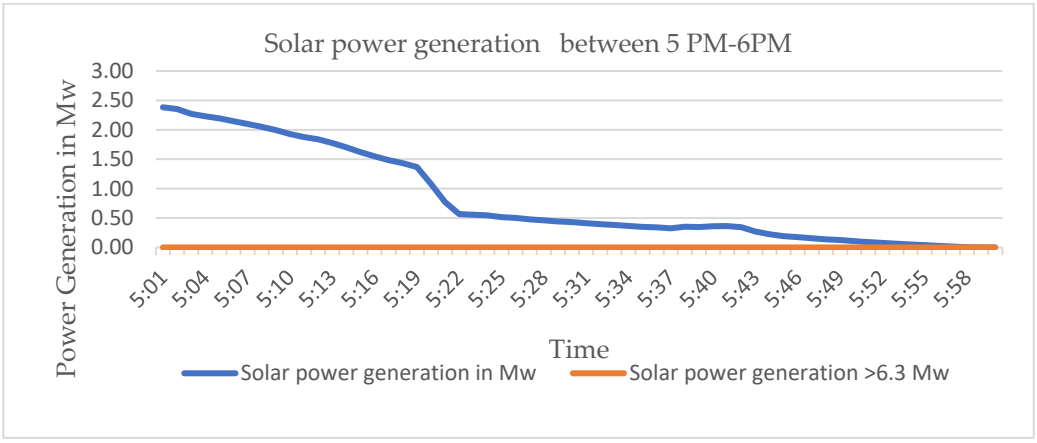

Figure 20. Solar generation between 5:00 p.m.–6:00 p.m.

From the above, solar generation is exceeding BEP for 7 h in a day, necessitating energy storage for 7 h only, and the total solar energy to be stored is 18.8 Mwh. For better life expectancy of the batteries, the considered batteries discharge up to 20% of capacity. Hence, the capacity of the batteries shall be 23.5 Mwh. Two battery banks are assumed, the capacity of each battery bank is 1.96 Mwh and the AH rating is 5800 based on 340 V DC. Hence, deep cycle tubular 2 V, 3000 AH @ C10 rating of two battery banks in parallel to each inverter is assumed. Figure 21 indicates the arrangement of the storage system proposed for the existing system.

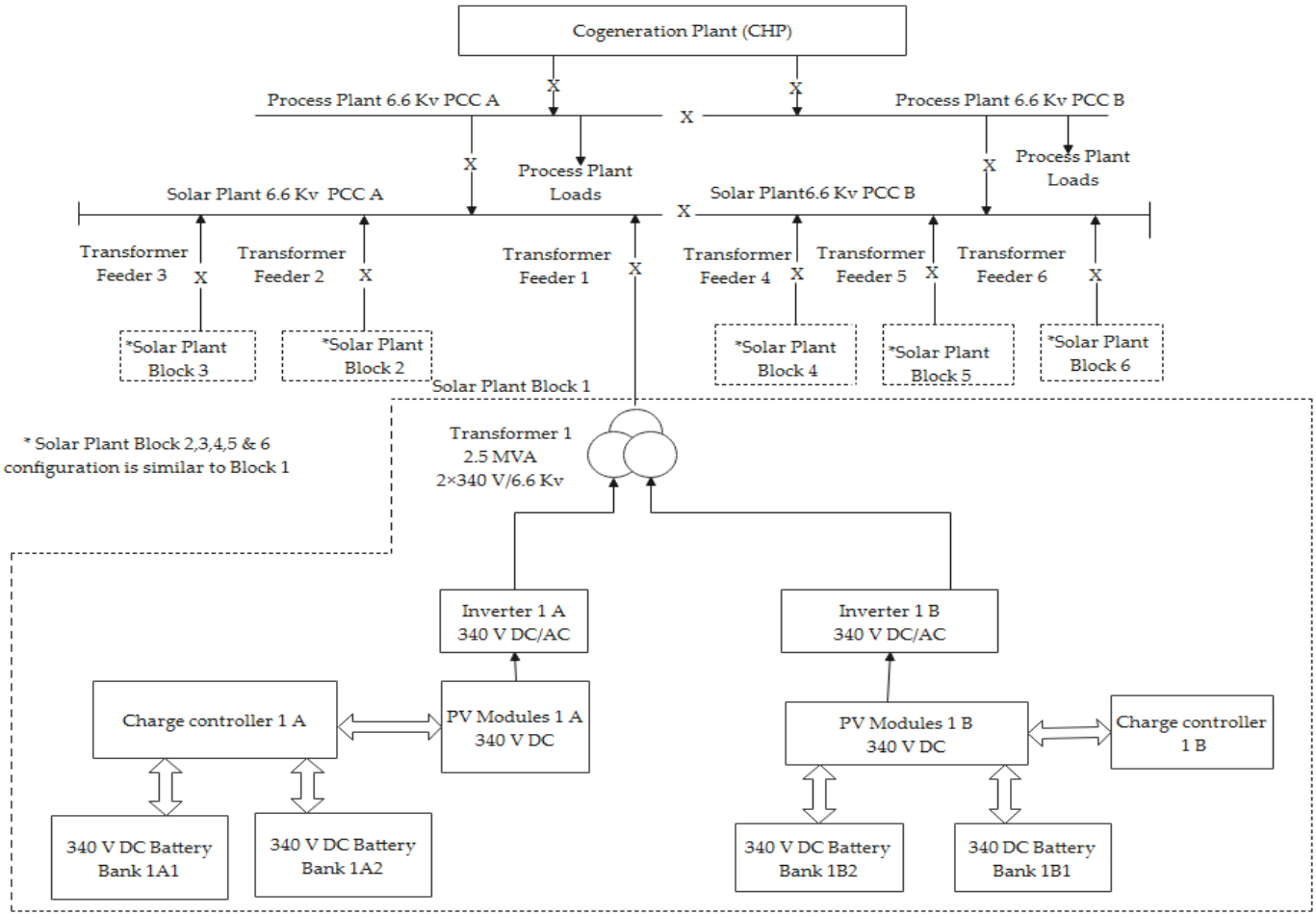

Figure 21. Block diagram of the cogeneration system with proposed battery energy storage.

With this rating, the 1 min charging data is verified, and the charging current does not exceed 600 amps except in a few instances which are also within 3% overload.

3.4.2. Control of Storage System

The storage system can be controlled based on the algorithm proposed in Figure 22. The charging of battery storage takes place whenever solar generation exceeds BEP. To have a simple control mechanism, the discharge is planned at the night for a period of 8 h. In the algorithm-developed discharge cycle is assumed for 8 h and the Discharge Timer (DT) gets switched on auto as per the time set, for example, 8 p.m. and discharge gets terminated as per the identified preconditions. The charging cycle will start based on the solar system's wake-up. To avoid intermediate switch over from the charging mode due to any partial cloudy conditions, the Charging Timer (CT) is preset to get switched off at 19.30 h after waking up in the morning. State of charge of batteries during charging time (SOC_{CT}) and during discharge time (SOC_{DT}) are considered based on battery charging current (I_{bc}) and battery discharging current (I_{bd}). Hence, the algorithm is developed to suit the present scenario, and the charging cycle and discharge cycle are made independent.

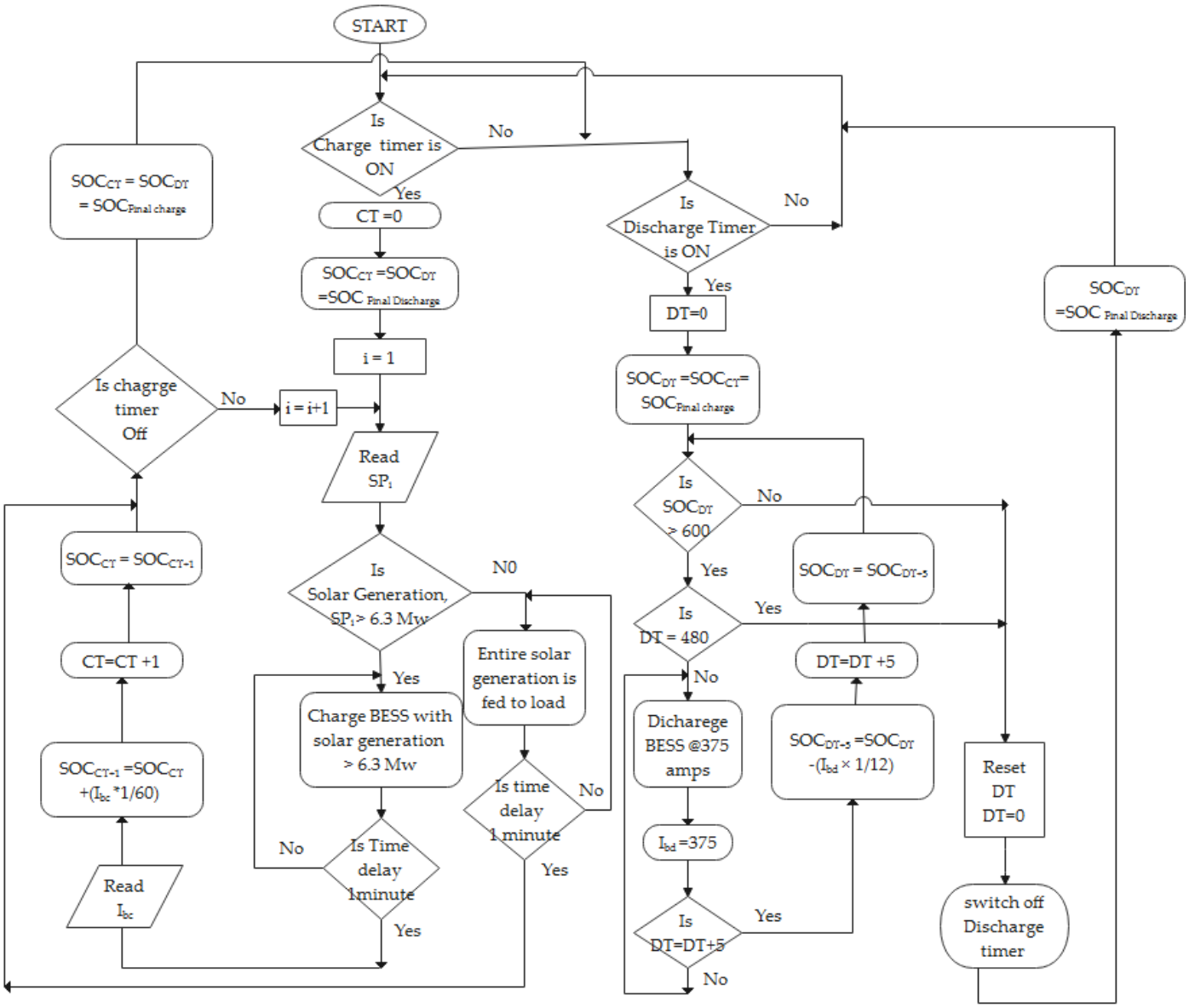

Figure 22. Control algorithm of Storage system.

4. Discussion

The computational complexity for optimization of a RE integrated cogeneration plant is simplified by analyzing the problem in steps. After identifying the optimality conditions responsible for deviation of the optimized operation of CHP plant with RE injection, BEP estimation becomes the initial starting point. Hence, two methods, i.e., practical experimentation and by using theoretical mathematical modeling are preferred. Mathematical equations developed are executed through MATLAB. Results obtained by both methods are discussed below.

The data obtained from the execution of the algorithm through MATLAB are compared with the practical data. The BEP is estimated as 6.3 Mw beyond which the SG flow is falling below a threshold limit of 320 MT/h. The practical values are compared with the developed algorithm values at 6.3 Mw. Values at 6.3 Mw were obtained through MATLAB interpolation coding. A comparison of results is represented in Table 15.

Table 15. Comparison of results with practical data.

S. No	Parameter	Unit	Comparison	
			MATLAB Interpolation Data	Practical Experimentation Data
			At 6.3 Mw	At 6.3 Mw
1	SG Flow	MT/h	320.9340	317
2	HP Extraction Flow	MT/h	210	210
3	LP Extraction Flow	MT/h	29.5343	27.8
4	HPPRDS Flow	MT/h	0	0
5	LPPRDS Flow	MT/h	5. 7	7.2
6	TG generation	Mw	24.7	25.5
7	Import/RE generation	Mw	6.3	6.3
8	Breakeven Point	Mw	6.8718	6.3

Figure 23 gives a comparative indication of BEP, TG generation, LPPRDS flow, and SG flow obtained through practical experimentation and mathematical modeling.

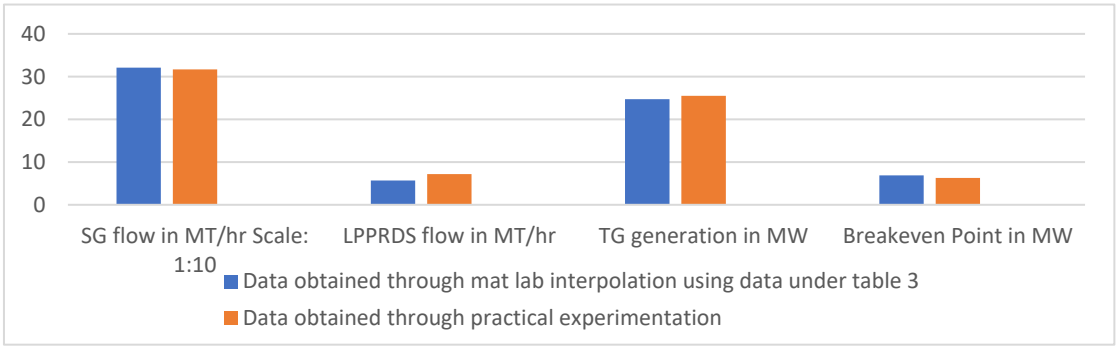

Figure 23. Comparison of parameters obtained through mathematical modeling and practical experimentation.

The above difference can be expected, as the SG and TG parameters cannot practically be kept constant and will always vary depending on many parameters like fuel quality, grid frequency, and process plant variations. Whereas these values are assumed constant during algorithm development. Hence both the methods based on suitability can be adopted by cogenerators. After BEP estimation adopting a suitable storage device for the present application is determined.

The methodology developed for the capacity determination of energy storage is a guide for RE integrated cogeneration plants. The control mechanism algorithm is developed to suit the present application. It is also found that the total charging of the designed battery bank in 7 h reaches around 77% i.e., indicating charging of the batteries from assumed 20% to 97%.

From Table 10, it can be observed that on a maximum solar radiation day, the total GTI is 6794.13 Wh/m^2/day and the expected solar generation is 74.64 Mwh. From Table 9, the total yearly GTI is 1825.82 kWh/m^2/year. Hence, the total Mwh generation in a year is 20,058.37 Mwh. Out of this, 50% of generation i.e., 10,029.19 Mwh, is unutilized, as 50% of the solar panels were switched off to maintain optimality conditions. Hence, by using energy storage, a net monetary benefit of Rs 5.0146 crores is envisaged. The expenditure can be 8.61 crores by considering the cost of 2 V, 3000 Ah cell @ Rs 20,000. Figure 24 indicates the comparison of monetary benefits due to RE utilization beyond BEP.

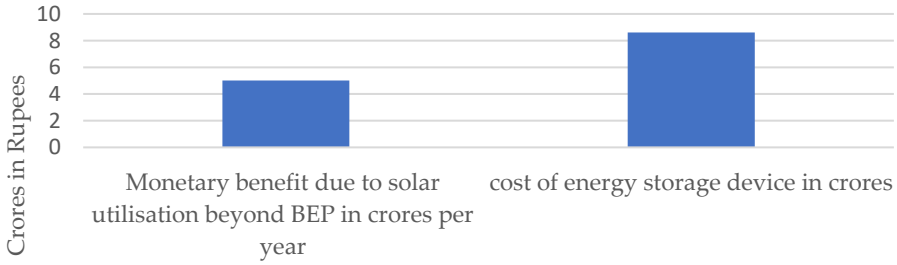

Figure 24. Comparison of monetary benefits due to RE utilisation beyond BEP.

Thus, the simple payback period is 1.72 years, which is well below the acceptable payback period of 3 years for any financing project. In addition to the financial savings, other benefits like meeting the RPPO obligations and reduction in CO_2 emissions strengthen the proposed scheme.

5. Conclusions

The post-operational constraints developed due to the integration of solar plant with existing cogeneration plant are effectively optimized by establishing BEP by practical and theoretical methods. Suitable storage device selected and capacity designed based on the available data. The control mechanism of the storage device is also proposed. The payback period of the storage system proposed is arrived at and proven economical. The methodology adopted in this paper is a guiding tool for designing storage systems for similar applications. Storage of energy will be a major issue in the future as future energy needs are by RE due to depletion of fossil fuels and associated environmental threats.

The outcome of this research presented a solution to the integration of renewable energy challenges faced by many industries. The energy share will definitely shift from the utilization of conventional fuels to renewables, which benefits society at large. This helps in improvement of energy security and sustainable growth, and at the same time protects the environment from further degradation.

Author Contributions: Data curation, Literature survey, research methodology, experimentation to estimate BEP, practical data collection, mathematical modeling, and algorithm development to estimate BEP on theoretical concepts, study on energy storage technologies, and determination of suitable technology, capacity, and sizing of the energy storage device, results and discussions and writing draft were carried out by A.V.R.N.B.M.R.; supervision, review, and editing were done by A.K.S. All authors have read and agreed to the published version of the manuscript.

Funding: This research received no external funding.

Institutional Review Board Statement: Not applicable.

Informed Consent Statement: Not applicable.

Data Availability Statement: Not applicable.

Conflicts of Interest: The authors declare no conflict of interest.

References

1. Manikyala Rao, A.; Singh, A.K.; Mrudula, A.S. Case study on Renewable energy integration (Solar) challenges with Captive/Cogeneration plants and optimization of plant operation. In Proceedings of the 3rd International Conference on Intelligent Circuits and Systems, (ICICS 2020), Punjab, India, 26–27 June 2020; pp. 11–19.
2. Shao, C.; Li, C.; You, X.; Wu, H.; Zhang, J.; Ding, Y.; Song, Y. Optimal coordination of CHP plants with renewable energy generation considering substitutability between electricity and heat. *Energy Procedia* **2016**, *103*, 100–105. [CrossRef]
3. Abdollahi, E.; Wang, H.; Rinne, S.; Lahdelma, R. Optimization of energy production of a CHP plant with heat Storage. In Proceedings of the IEEE Green Energy and Systems Conference (IGESC 2014), Long Beach, CA, USA, 24 November 2014; pp. 30–34.
4. Kahlert, S.; Spliethoff, H. Investigation of different operation strategies to provide Balance Energy with an Industrial Combined Heat and Power Plant using Dynamic Simulation. *J. Eng. Gas Turbines Power* **2017**, *139*, 011801-1–011801-8. [CrossRef]
5. Werner, F.; Burtseva, L.; Sotskov, Y.N. Special Issue on Exact and Heuristic Scheduling Algorithms. *Algorithms* **2020**, *13*, 9. [CrossRef]
6. Cagri, K.; Eren, O.; Saadettin, E.K.; Zeynel, A.C.; Suleiman, M. Forward supply chain network design problem: Heuristic approaches. *Pamukkale Univ. J. Eng. Sci.* **2018**, *24*, 749–763.
7. Saxena, D.; Malik, N.K.; Singh, V.R. A cognitive approach to solve water jugs problem. *Int. J. Comput. Appl.* **2015**, *124*, 45–54. [CrossRef]
8. Kumar, J.N.; Suryanarayanan, R.; Chitra, P.; Dharmalingam, P.; Prabhu, H.R.; Velayutham, V. Co-generation. In *Guidebook 2 for National Level Certification Examination for Energy Managers and Energy Auditors—Energy Efficiency in Thermal Utilities*, 4th ed.; Bureau of Energy Efficiency: New Delhi, India, 2015; Chapter 7, pp. 189–214.
9. Kumar, J.N.; Suryanarayanan, R.; Chitra, P.; Dharrmalingam, P.; Prabhu, H.R.; Velayutham, V. Energy performance assessment of cogeneration systems. In *Guidebook 4 for National Level Certification Examination for Energy Managers and Energy Auditors—Energy Performance Assistance for Equipment and Utility Systems*, 4th ed.; Bureau of Energy Efficiency: New Delhi, India, 2015; Chapter 3, pp. 41–52.
10. Rout, I.S.; Gaikwad, A.; Verma, V.K.; Tariq, M. Thermal Analysis of Steam Turbine Power Plants. *IOSR J. Mech. Civ. Eng.* **2013**, *7*, 28–36. [CrossRef]
11. Sumanta Basu. Modeling of Steam Turbine Generators from Heat Balance Diagram and determination of frequency response. *Control Sci. Eng.* **2018**, *2*, 1–15. [CrossRef]
12. More, P.S.; Aijaz, A. Thermal Analysis of Energy and Exergy of Back Pressure Steam Turbine in Sugar Cogeneration Plant. *Int. J. Emerg. Technol. Adv. Eng.* **2014**, *4*, 674–682.
13. Kumar, J.N.; Suryanarayanan, R.; Chitra, P.; Dharmalingam, P.; Prabhu, H.R.; Velayutham, V. Financial Management. In *Guidebook 1 for National Level Certification Examination for Energy Managers and Energy Auditors—General Aspects of Energy Management and Energy Audit*, 4th ed.; Bureau of Energy Efficiency: New Delhi, India, 2015; Chapter 7, pp. 163–188.
14. Pascual, N.; Sison, A.M.; Gerardo, B.D.; Medina, R. Calculating Internal Rate of Return (IRR) in Practice using improved Newton Raphson's Algorithm. *Philipp. Comput. J.* **2018**, *13*, 17–24.
15. Gustavsson, J. Energy Storage Technology Comparison—A Knowledge Guide to Simplify Selection of Energy Storage Technology. Bachelor's Thesis, KTH School of Industrial Engineering and Management Energy Technology, Stockholm, Sweden, 2016; pp. 1–36.
16. Sharma, S.S.; Kumar, V.; Joshi, R.R. An Overview on Energy Storage Options for Renewable Energy Systems. In Proceedings of the National Conference, ITM, Bhilwara, Rajasthan, 10–11 September 2010.
17. Hussein, I.; Adrian, I. Techno Economic Analysis of Different Energy Storage Technologies. In *Energy Storage-Technologies and Applications*; Intech Open: London, UK, 2013; Chapter 1, pp. 1–40. [CrossRef]
18. Bartek, A.G.; Emma, S.H. Energy Storage Technology for Decentralized Energy Management: Future Prospects. In *Energy Management of Distributed Generation Systems*; Intech Open: London, UK, 2016; Chapter 8, pp. 183–200. [CrossRef]
19. Grigorios, L.K.; Garyfallos, A. Electrical energy storage systems in electricity generation: Energy policies, innovative technologies, and regulatory regimes. *Renew. Sustain. Energy Rev.* **2016**, *56*, 1044–1067. [CrossRef]
20. Annette, E.; Vladimir, S.; Tim, J.E. Assessment of utility energy storage options for increased renewable energy penetration. *Renew. Sustain. Energy Rev.* **2012**, *16*, 4141–4147. [CrossRef]
21. Surender, R.S.; Chan-Mook, J. Comparative analysis of storage techniques for a grid with renewable energy sources. *Int. J. Eng. Technol.* **2018**, *7*, 970–976. [CrossRef]
22. Ghenai, C.; Janajreh, I. Comparison of energy storage options and determination of suitable technique for solar power systems. In Proceedings of the SASEC2015 Third Southern African Solar Energy Conference, Skukuza, South Africa, 11–13 May 2015; pp. 204–210.
23. Henok, A.B.; Maarten, M.; Thierry, C.; Maitane, B.; Kinde, A.F.; Abraham, A.K.; Joeri, V.M. A Review of Energy Storage Technologies Application Potentials in Renewable Energy Sources Grid Integration. *Sustainability* **2020**, *12*, 10511. [CrossRef]
24. Dimitris, K.; Irini, D. Comparing electricity storage technologies for small insular grids. *Sci. Direct Energy Procedia* **2019**, *159*, 84–89.
25. Upendra Roy, B.P.; Rengarajan, N. Feasibility study of an energy storage system for distributed generation system in islanding mode. *J. Energy Resour. Technol.* **2017**, *139*, 011901. [CrossRef]

26. Behnam, Z.; Sanna, S. Electrical energy storage systems: A comparative life cycle cost analysis. *Renew. Sustain. Energy Rev.* **2015**, *42*, 569–596.
27. Patrik, L.; Philip, B. Cost models for Battery Energy Storage Systems. Bachelor's Thesis, KTH School of Industrial Engineering and Management Energy Technology, Stockholm, Sweden, 2018; pp. 1–28.
28. Pellow, M.A.; Emmott, C.J.; Barnhart, C.J.; Benson, S.M. Hydrogen or batteries for grid storage? A net energy analysis. *Energy Environ. Sci. R. Soc. Chem.* **2015**, *8*, 1938–1952. [CrossRef]
29. Barnhart, C.J.; Dale, M.; Brandt, A.R.; Benson, S.M. The energetic implications of curtailing versus storing solar and wind generated electricity. *Energy Environ. Sci.* **2013**, *6*, 2804–2810. [CrossRef]
30. Moien, A.O.; Marwan, M.M. Design and Simulation of a PV System Operating in Grid-Connected and Stand-Alone Modes for Areas of Daily Grid Blackouts. *Int. J. Photo Energy* **2019**, *2019*, 5216583. [CrossRef]
31. Purnima, P.; Ravendra, G.; Srinivas, J. Power and Energy Rating Considerations in Integration of Flow Battery with Solar PV and Residential Load. *Batteries* **2021**, *7*, 62. [CrossRef]
32. Chung, M.H. Estimating Solar Insolation and Power Generation of Photovoltaic Systems Using Previous Day Weather Data. *Adv. Civ. Eng.* **2020**, *2020*, 8701368. [CrossRef]
33. Nurul, A.; Naamandadin; Chew, J.M.; Wan, A.; Mustafa. Relationship between Solar Irradiance and Power Generated by Photovoltaic Panel: Case Study at UniCITI Alam Campus, Padang Besar, Malaysia. *J. Adv. Res. Eng. Knowl.* **2018**, *5*, 16–20.
34. Akif, K.; Harun, O.; Metin, K. Temperature and Solar Radiation Effects on Photovoltaic Panel Power. *J. New Results Sci.* **2016**, *12*, 48–58.
35. Nahidul, H.S.; Norhafizan, B.A.; Imtiaz, A.C.; Zahari, B.T. Modeling, Control, and Simulation of Battery Storage Photovoltaic-Wave Energy Hybrid Renewable Power Generation Systems for Island Electrification in Malaysia. *Sci. World J.* **2014**, *2014*, 436376.
36. Aastha, K.; Sharma, A. Optimal Charge/Discharge Scheduling of Battery Storage Interconnected with Residential PV System. *IEEE Syst. J.* **2019**, *14*, 3825–3835.
37. Ayman, B.A.; Adam, V. Operation and Control of a Hybrid Power Plant with the Capability of Grid Services Provision. *Energies* **2021**, *14*, 3928. [CrossRef]
38. Imene, Y.; Natalia, V.D.L.P. Energy Management Strategy for an Autonomous Hybrid Power Plant Destined to Supply Controllable Loads. *Sensors* **2022**, *22*, 357. [CrossRef]
39. Sercan, T.; Mesut, E.B.; Subhashish, B.; Alex, Q.H. Rule-Based Control of Battery Energy Storage for Dispatching Intermittent Renewable Sources. *IEEE Trans. Sustain. Energy* **2010**, *1*, 117–124.